The Genesis of Hurricane Guillermo: TEXMEX Analyses and a Modeling Study

MARJA BISTER AND KERRY A. EMANUEL

Center for Meteorology and Physical Oceanography, Massachusetts Institute of Technology, Cambridge, Massachusetts

(Manuscript received 29 October 1996, in final form 6 December 1996)

ABSTRACT

The transformation of a mesoscale convective system into Hurricane Guillermo was captured by aircraft and Doppler wind data during the Tropical Experiment in Mexico. The early phase of the system evolves in a way very similar to previously documented mesoscale convective systems, with a midlevel mesocyclone developing in the stratiform precipitation region. More unusually, the cyclone extends to low altitudes: A weak cyclone is discernable even in the 300-m altitude wind field. After another day of evolution, a small, surface-based warm-core cyclone is observed to develop within the relatively cold air associated with the mesocyclone aloft. This mesocyclone develops into a hurricane over the subsequent day.

A nonhydrostatic, axisymmetric numerical model is used to explore the evolution of the initially cold-core, midlevel vortex into a tropical cyclone. A mesoscale, midlevel ''showerhead'' is switched on in an initially quiescent, tropical atmosphere overlying a warm ocean surface. Evaporation of the falling rain cools the lower troposphere and leads to the spinup of a midlevel vortex, while divergent outflow develops near the surface. After some time, the midlevel vortex expands downward toward the boundary layer, and later a warm-core, surface-flux-driven cyclone develops within it. Experiments with the model show that both the cyclone, with its associated cold anomaly, and the relatively humid air associated with the evaporatively cooled mesoscale cyclone are important for the subsequent development of the warm-core system. The simulations also suggest that, for the warm-core development to occur, the stratiform rain must last long enough to drive the midlevel vortex down to the boundary layer. The authors present a simple argument for why this must be so and suggest that this process would be significantly impeded by the presence of background vertical wind shear.

1. Introduction

It has been known for more than 50 years that tropical cyclones do not form spontaneously. Rotunno and Emanuel (1987, hereinafter RE) suggested that incipient disturbances are prevented from developing by convective downdrafts in their cores, which bring air of low equivalent potential temperature (Θ_e) into the boundary layer, suppressing further convection. Therefore, for tropical cyclogenesis to occur, the negative effect of the downdrafts has to be overcome. In principle, this might happen through an increase of the equivalent potential temperature in the middle troposphere, an increase of relative humidity so that evaporation of rain is suppressed, and/or an increase of wind speed so that the sea surface fluxes keep replenishing the boundary layer Θ_e. The simulations by RE and Emanuel (1989), in which a warm-core vortex was used in the initial state, suggested that an increase of Θ_e in the middle troposphere is necessary for tropical cyclogenesis. The main goal of the Tropical Experiment in Mexico (TEXMEX) was to test a hypothesis stated in the TEXMEX Operations Plan (available from the second author): The elevation of Θ_e in the middle troposphere just above a near-surface vorticity maximum is a necessary and perhaps sufficient condition for tropical cyclogenesis. It was assumed that the elevation of Θ_e is accomplished by deep convection bringing high Θ_e to the middle troposphere, as occurs in the models initialized by warm-core vortices.

The objective of this paper is to present a case study of tropical cyclogenesis during TEXMEX, to use it to test the aforementioned hypothesis, and to develop a new theory of tropical cyclogenesis. The case in question is a weather disturbance that developed into Hurricane Guillermo during TEXMEX in 1991.

The organization of this paper is as follows. In section 2 we present an overview of TEXMEX and the particular case that constitutes the subject of this paper. In section 3, the data and analysis methods are discussed. The analysis and interpretation of the analysis results, with references to earlier work, are presented in section 4. We postulate a mechanism for the development of Hurricane Guillermo and test it using a numerical model that is described in section 5. Results from the numerical simulations are presented in sections 6 and 7. A thought experiment that concerns an important aspect of tropical cyclogenesis is presented in section 8, and results are summarized in section 9.

Corresponding author address: Marja Bister, Finnish Meteorological Institute, P.O. Box 503, 00101 Helsinki, Finland.
E-mail: bister@cirrus.mit.edu, marja.bister@fmi.fi

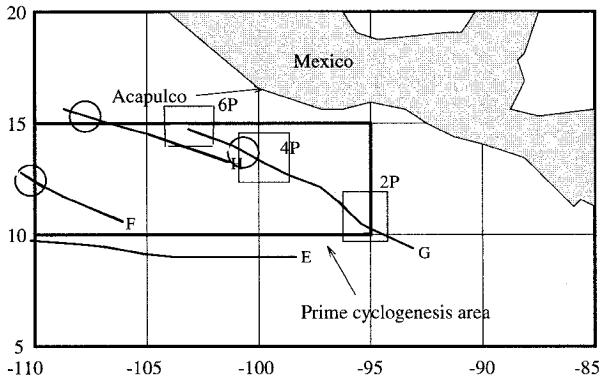

FIG. 1. Tracks of aircraft-estimated vortex centers of TEXMEX cases that developed into hurricanes (from D. Raymond). Circles show where each disturbance was declared a tropical storm by the National Hurricane Center: E = Enrique, F = Fefa, G = Guillermo, H = Hilda. Here, 2P, 4P, and 6P denote the location of the vortex associated with (pre-)Guillermo MCS during these flights (see sections 3 and 4). Boxes show the regions surveyed during these three flights.

2. Overview of TEXMEX and the mesoscale convective system leading to Hurricane Guillermo

TEXMEX was designed to observe intensively the process of tropical cyclogenesis, with the principal aim of testing the aforementioned hypothesis about how genesis takes place. This hypothesis was tested by making measurements inside developing and nondeveloping cloud clusters, using the WP-3D aircraft operated by the National Oceanic and Atmospheric Administration's (NOAA) Office of Aircraft Operations and the National Center for Atmospheric Research (NCAR) Lockheed Electra. Both aircraft were equipped to make in situ measurements of standard meteorological variables, and the WP-3D had the additional capability of deploying Omega dropwinsondes (ODW) and making detailed Doppler radar measurements. Details of the aircraft measurement systems are described in the TEXMEX Operations Plan.

The eastern tropical North Pacific region was selected for the field program as it has the highest frequency of genesis per unit area of any region worldwide (Elsberry et al. 1987) and the main genesis region is only a few hundred kilometers south of Acapulco, Mexico, which has an airport well suited to research flight operations. The field phase of the experiment began on 1 July and ended on 10 August 1991. During the project there were six intensive operation periods (IOPs) that surveyed one short-lived convective system, one nondeveloping mesoscale convective system (MCS), and four MCSs that ultimately developed into hurricanes. The tracks of those systems that developed into hurricanes are shown in Fig. 1. Detailed description of the aircraft flight operations are provided in the TEXMEX Data Summary (available from the second author).

As the principal working hypothesis concerned thermodynamic transformations of the lower and middle troposphere, most flight operations were conducted near the 700-mb level and in the subcloud layer. The tail Doppler radar on the WP-3D operated almost uninterrupted through all of the flight operations. In order to maximize the temporal continuity of observations of evolving cloud clusters, while obeying operational constraints, the aircraft flew alternating missions at approximately 14-h intervals. Most flight missions lasted 7–9 h, of which 1–3 h were used in transit to the target area.

Molinari et al. (1997) noted that the 1991 hurricane season over the eastern North Pacific consisted of several active and inactive periods of cyclogenesis. Hurricane Guillermo developed during one of the active periods. The sequence of events leading to Hurricane Guillermo began with the development of an MCS. In Fig. 2 satellite images from the MCS are shown at various times before tropical-storm strength was reached. The MCS developed over the Honduras–El Salvador border during the night of 1–2 August 1991, with convection developing rapidly into a north-northeast–south-southwest-oriented line extending southward from the coast as shown in Fig. 2a (0800 UTC 2 August). Four hours later, however, the MCS had lost its linelike appearance (Fig. 2b, 1200 UTC), and after 8 h, the satellite imagery shows a line of convection propagating to the west and leaving behind the rest of the MCS (Fig. 2c, 2000 UTC).

The MCS developed while an easterly wave was propagating into the eastern Pacific from the Caribbean Sea (Farfan and Zehnder 1997, FZ hereinafter). This easterly wave can be seen over and to the southwest of Cuba in the European Centre for Medium-Range Weather Forecasts (ECMWF) 700-hPa wind analysis at 0000 UTC 3 August 1991 (Fig. 3). The satellite image 4 h after the time of the wind analysis and 8 h after the third satellite image (Fig. 2d, 0400 UTC 3 August) shows weaker convection, with the line of convection propagating farther from the rest of the MCS. After this minimum of convection, probably associated with the diurnal cycle, convection starts to intensify. The intensified convection 12 h later can be seen in Fig. 2e (1600 UTC). After another 16 h (Fig. 2f, 0800 UTC 4 August), strong cells are developing in the center of the MCS, and within 10 h (1800 UTC 4 August) the system had reached tropical storm strength. After another 16 h, at 1000 UTC 5 August, the storm was upgraded to a hurricane.

3. Data and analysis methods

The pre-Guillermo MCS was the object of IOP 5 from 2 August 1991 to 5 August 1991, during which six flights were flown. The first, third, and fifth flights, labeled 1E, 3E, and 5E, respectively, were flown with the Electra while the second, fourth, and sixth flights, labeled 2P, 4P, and 6P, respectively, were flown with the

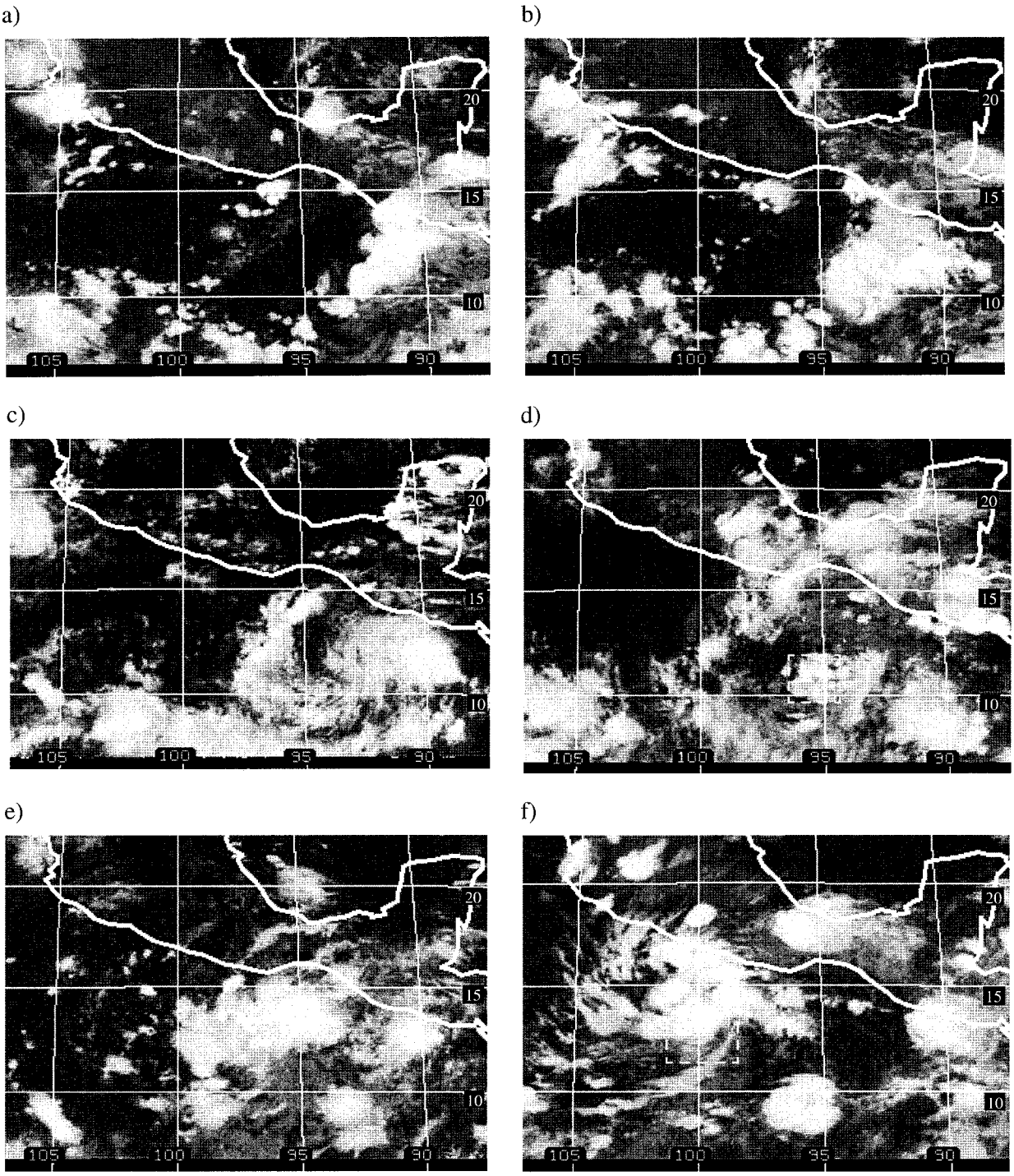

FIG. 2. GOES infrared image at (a) 0800 UTC 2 August, (b) 1200 UTC 2 August, (c) 2000 UTC 2 August, (d) 0400 UTC 3 August, (e) 1600 UTC 3 August, and (f) 0800 UTC 4 August. The area surveyed by the P3 aircraft during flights 2P and 4P is shown with boxes in (d) and (f), respectively.

WP-3D. These flights are summarized in Table 1. Each flight consisted of several flight legs at both 3-km and 300-m altitudes.

In the stratiform precipitation areas, measurements made by the ODWs often showed 100% relative humidity, indicating wetting of the instruments. For this reason, the ODW data were not used in our analysis. Radar composites from the WP-3D C-band radar provide an overview of convection during the flights. Geostationary Operational Environmental Satellite

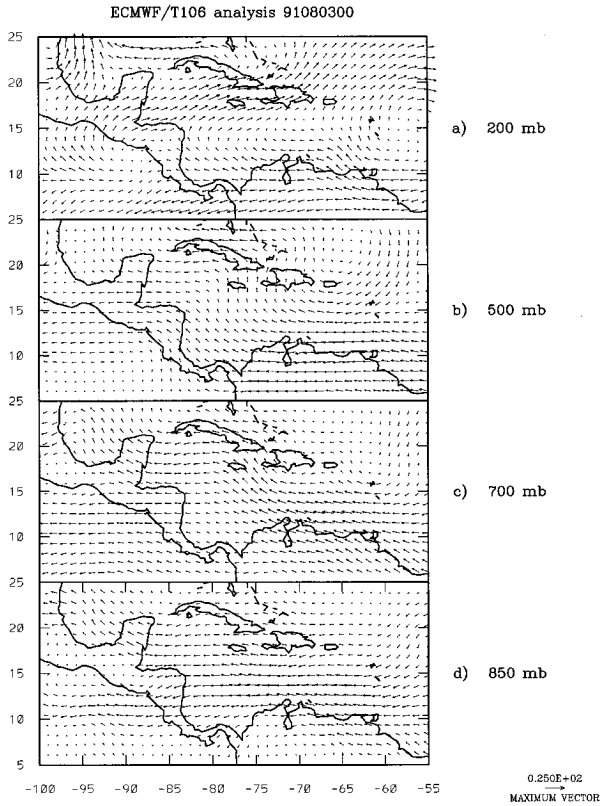

FIG. 3. ECMWF wind analysis at 0000 UTC 3 August 1991. Analyses courtesy of Farfán and Zehnder.

(GOES) imagery and analysis of winds from the ECMWF were obtained from L. Farfán and J. Zehnder of the University of Arizona.

a. Doppler radar data

The Doppler radar data we analyzed were collected when the aircraft was flying at 3-km altitude. In general, adequate reflectors were present up to at least 7 km because of widespread stratiform precipitation. The general characteristics of the radar are described in Marks and Houze (1987). The Doppler radar was used in the fore–aft scanning technique mode (Gamache et al. 1995), in which the radar antenna scans two cones about the aircraft's longitudinal axis. The Doppler radar data were prepared for analysis as follows. First, the components of the aircraft's ground velocity and precipitation fallspeed (see Marks and Houze 1987) in the direction of the antenna were subtracted from the velocity measurement. The velocities were then unfolded automatically using Bargen and Brown's method (1980). Manual editing of the data followed the automatic unfolding, and unrealistic wind data were deleted. Most of the data deleted were from 0.5-, 1.0-, and 1.5-km altitudes. Data from these altitudes appear to have been compromised by sea clutter. Finally, the three-dimensional wind was calculated iteratively from the two radial components using the continuity equation.

Both the in situ and the Doppler data were gathered over the 4–6-h time period during which the aircraft was surveying the system. A correction was made for the movement of the MCS by using a translation velocity, estimated by tracking the vortex center from one flight to the next, to move each data point to an appropriate position at some reference time.

We assess the accuracy of the Doppler wind data by comparing the easterly and northerly Doppler wind components to the in situ wind components. The mean difference is less than 2 m s^{-1} and the standard deviation is less than 2.5 m s^{-1}; however, errors in the Doppler winds owing to errors in the estimated precipitation fallspeed and the measured ground speed of the aircraft cannot be assessed by this comparison. The error in the measured ground speed is about 2–3 m s^{-1} (B. Damiano 1992, personal communication), introducing a Doppler velocity error that is constant with height. The errors in the wind associated with the terminal fallspeed were estimated to be less than 1 m s^{-1} for horizontal distances of more than 4 km from the flight track.

b. In situ data

Intercomparisons of instruments onboard the NOAA WP-3D and the NCAR Electra were made using data from two sets of intercomparison flights in the beginning and at the end of the field experiment. The differences of the temperature and the dewpoint temperature measured by the two aircraft were less than 0.3 K during both flights, and they were accounted for in the data analysis. Data were excluded from the analysis if the magnitude of the vertical velocity exceeded 1 m s^{-1}, in order to minimize the effect of active convective updrafts and downdrafts on the analyzed fields. Data were

TABLE 1. Summary of flights into (pre-)Guillermo: F is following day, TS is tropical storm, and H is hurricane.

Flight	Target	Date	Time (UTC) at 700 hPa	Time (UTC) at 300 m
1E	—	2 Aug 1991	—	—
2P	Pre-Guillermo	2 Aug 1991	0119–0412 F	0419–0610 F
3E	Pre-Guillermo	3 Aug 1991	1510–1810	1824–1930
4P	Pre-Guillermo	4 Aug 1991	0445–0737	0748–1001
5E	TS Guillermo	4 Aug 1991	1830–2140	2150–0005 F
6P	H Guillermo	5 Aug 1991	0750–0900	1100–1300

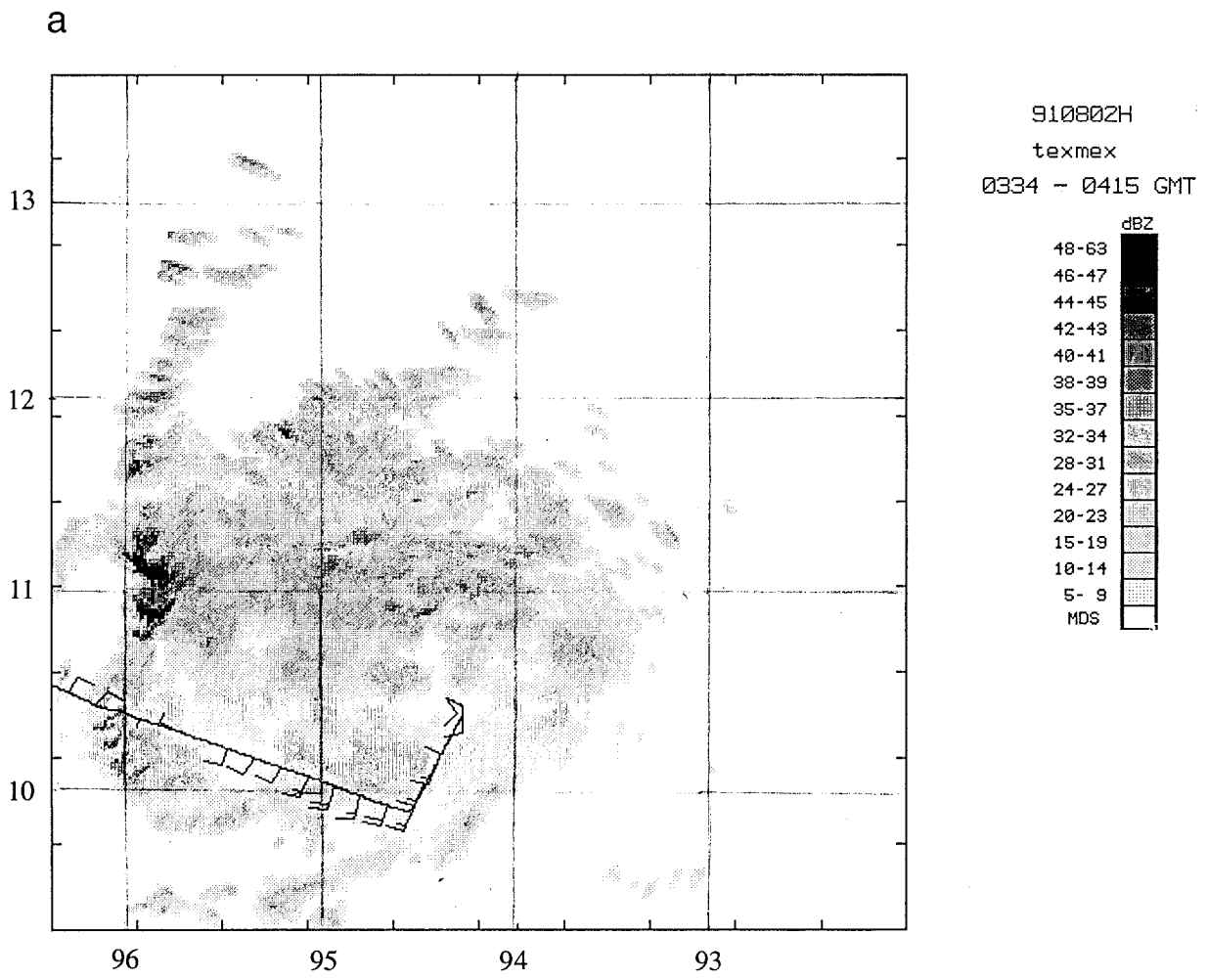

FIG. 4. Pre-Guillermo mesoscale system during flight 2P. (a) Composite of radar reflectivity (dBZ) from the 3-km altitude. (b) Wind from Doppler radar at 2 km. Long barb is 10 m s^{-1}; short barb 5 m s^{-1}. (c) Virtual potential temperature (K, solid) and relative humidity (%, gray shading) at 3 km. (d) Change of Doppler wind from the 1 to 3-km altitudes; only values larger than 3 m s^{-1} are plotted.

also excluded if the measured dewpoint temperature exceeded the measured temperature. However, no data were excluded from the 300-m analyses or from flight 6P. Using the same method as with the Doppler data, the data were renavigated to the appropriate locations at a given time, and 80-s (10-km) averages were calculated. These averages were then analyzed by hand.

4. Analysis results and interpretation

In the following, we discuss the analysis of observations from flights 2P, 4P, and 5E conducted at around 0200 UTC 3 August, 0600 UTC 4 August, and 2000 UTC 4 August, respectively. (The first flight, 1E, was conducted well to the west of the developing system.) The large-scale flow features associated with the MCS, particularly the easterly wave shown in Fig. 3, have been described in detail in FZ.

Figure 2d shows that flight 2P was conducted in what seems to be the trailing part of the earlier linear convection (Figs. 2a–c). Figure 4a shows the radar reflectivity in the MCS. Apart from the bands of deep convection with high radar reflectivity to the north and west, the convection is mainly stratiform with a well-defined bright band at the altitude of 4.4 km (not shown). Figure 4b shows the simultaneous Doppler radar wind at 2-km altitude. A mesoscale cyclonic vortex can be seen centered between 10° and 11°N and 95° and 96°W. Comparison of Figs. 4a and 4b shows that the vortex is in the stratiform region of the precipitation. Doppler winds at 1-km altitude (not shown) show the mesoscale vortex in the same location, associated with a negative pressure anomaly (not shown), but with weaker winds than at 2-km altitude. The relative humidity at 3-km altitude (Fig. 4c) varies mostly between 80% and 90% with peak values in the region of the vortex core. The analysis of virtual potential temperature at 3 km (Fig. 4c) suggests a lower-trospospheric cold core associated with the vor-

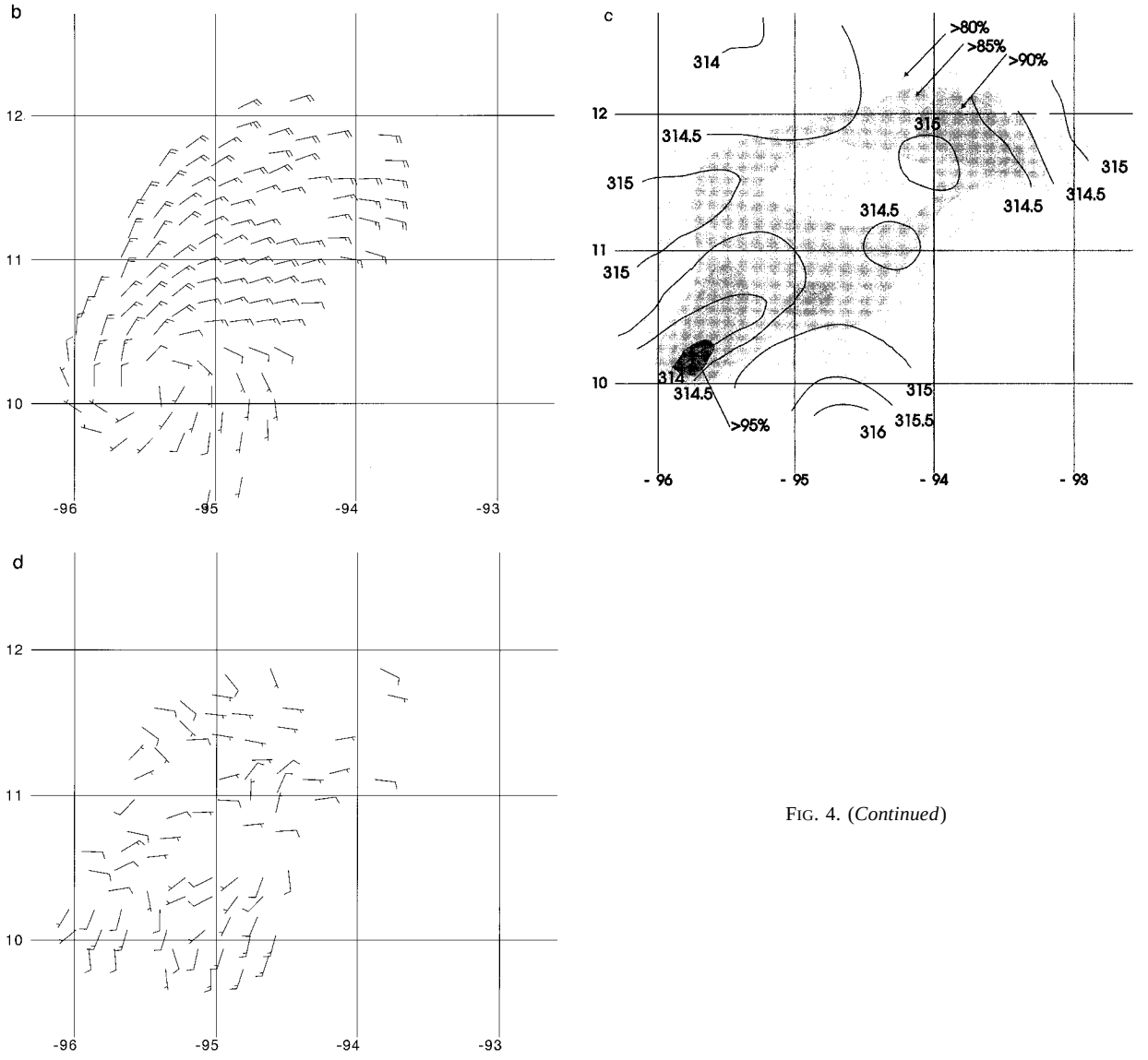

FIG. 4. (*Continued*)

tex at this altitude. The Doppler wind field can be used to determine whether the cold core extends to a deeper layer because, assuming that the vortex is in balance with the thermal field, the change of wind with altitude is a proxy for the thermal anomalies in the corresponding layer. Therefore, if the wind shear is anticyclonic (cyclonic), the vortex has a warm (cold) core. The vertical difference between the wind at 3 and 1 km (Fig. 4d) suggests a cold core in the lower troposphere associated with the vortex. A warm core in the upper troposphere is suggested by the wind change between 5 and 7 km (not shown). The equivalent potential temperature varies by no more than 4 K in the region shown in Fig. 4c, with the highest values of 339 K collocated with the center of the vortex (not shown).

During flight 4P, 28 h later, the highest radar reflectivity (Fig. 5a), indicating bands of deep convection, still lies mostly on the northern and western sides of the 2-km vortex center located at 13.1°N, 99.1°W (Fig. 5b). The satellite image (Fig. 2f) shows that strong deep convection was developing in the center of the flight pattern 2 h after the time of the radar reflectivity analysis in Fig. 5a. The analysis of virtual potential temperature now shows a small local maximum inside the cold core at both 3-km and 300-m altitudes (Fig. 5c). The change of the Doppler wind between the 1.5- and 4.5-km altitudes is shown in Fig. 5d and is consistent with the virtual potential temperature distribution at 3 km (Fig. 5c). The vertical wind shear is generally cyclonic, indicating a cold core, but there is a small region with anticyclonic wind shear collocated with the local temperature maximum evident in Fig. 5c. Note that the warm core is developing near the region of the developing strong convection apparent in Fig. 2f. This is also

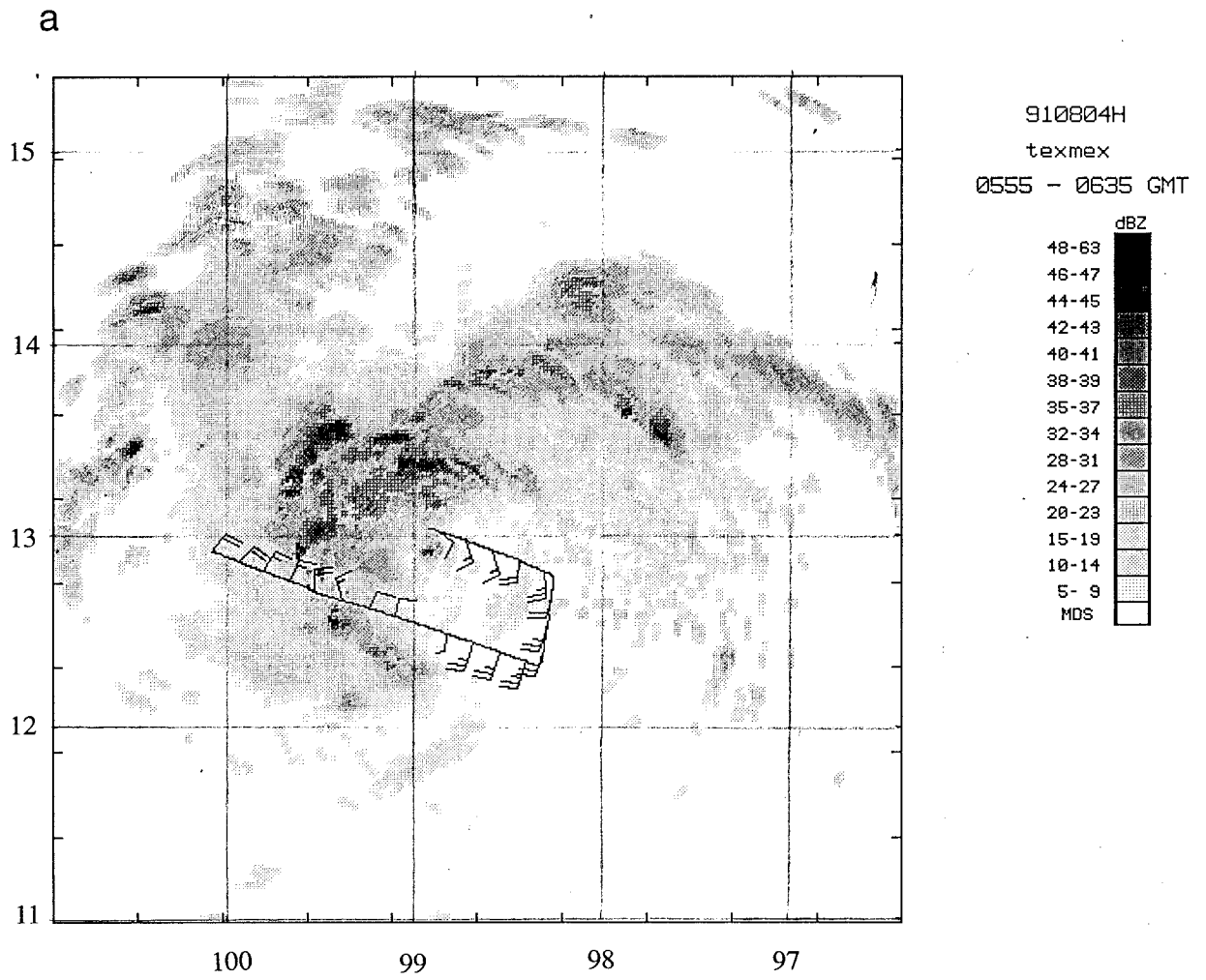

FIG. 5. Pre-Guillermo mesoscale system during flight 4P. (a) Composite of radar reflectivity from the 3-km altitude. (b) Wind from Doppler radar at 2 km. (c) Virtual potential temperature at the 3-km altitude (contours) and at 300 m (gray shading). (d) Change of Doppler wind from 1.5 to 4.5 km; only values larger than 4.5 m s^{-1} are plotted. Units as in Fig. 4.

the location where the surface wind speed (not shown) is largest.

Figure 6a shows the in situ winds at 3-km altitude 14 h later during flight 5E. The system is of tropical storm strength now, with maximum wind exceeding 17 m s^{-1}. The warm core at 3-km altitude is now dominant, but there is still a reversal of the gradient of the virtual potential temperature about 100 km from the center of the warm core (Fig. 6b). This reversal is also found in the boundary layer (not shown).

The last flight of IOP 5 began 14 h after flight 5E. At the time of this flight, by 1200 UTC 5 August, the system was a hurricane with a maximum wind speed of about 35 m s^{-1}.

To get a rough picture of thermodynamic changes in the region of the vortex, we calculate averages of the virtual potential temperature, Θ_e, and relative humidity in boxes of roughly 140 km $\times$ 140 km centered at the vorticity maximum in the lower troposphere. These averages were calculated for flights 2P, 4P, and 6P and are shown in Table 2. (Note that data from flight 6P instead of 5E are used here. Thus, the time difference between each pair of consecutive flights in Table 2 is about 28 h.) Note that there is little change in the relative humidity, Θ_e, and virtual potential temperature at 3-km altitude, between flights 2P and 4P. However, the boundary layer relative humidity increases by 7% and Θ_e increases by 3 K between these flights. This suggests that between the cold-core stage and the development of the central warm core the system's main thermodynamic change is moistening of the boundary layer. (These results are not sensitive to displacing the boxes by 15 km, but are sensitive to displacing the boxes by 50 km.) The transition to a hurricane is associated with an increase of Θ_e of about 5 K in both the boundary layer and at 3-km altitude, and an increase of virtual potential temperature of about 2–3 K at both altitudes. The increase of Θ_e and virtual potential temperature in both the

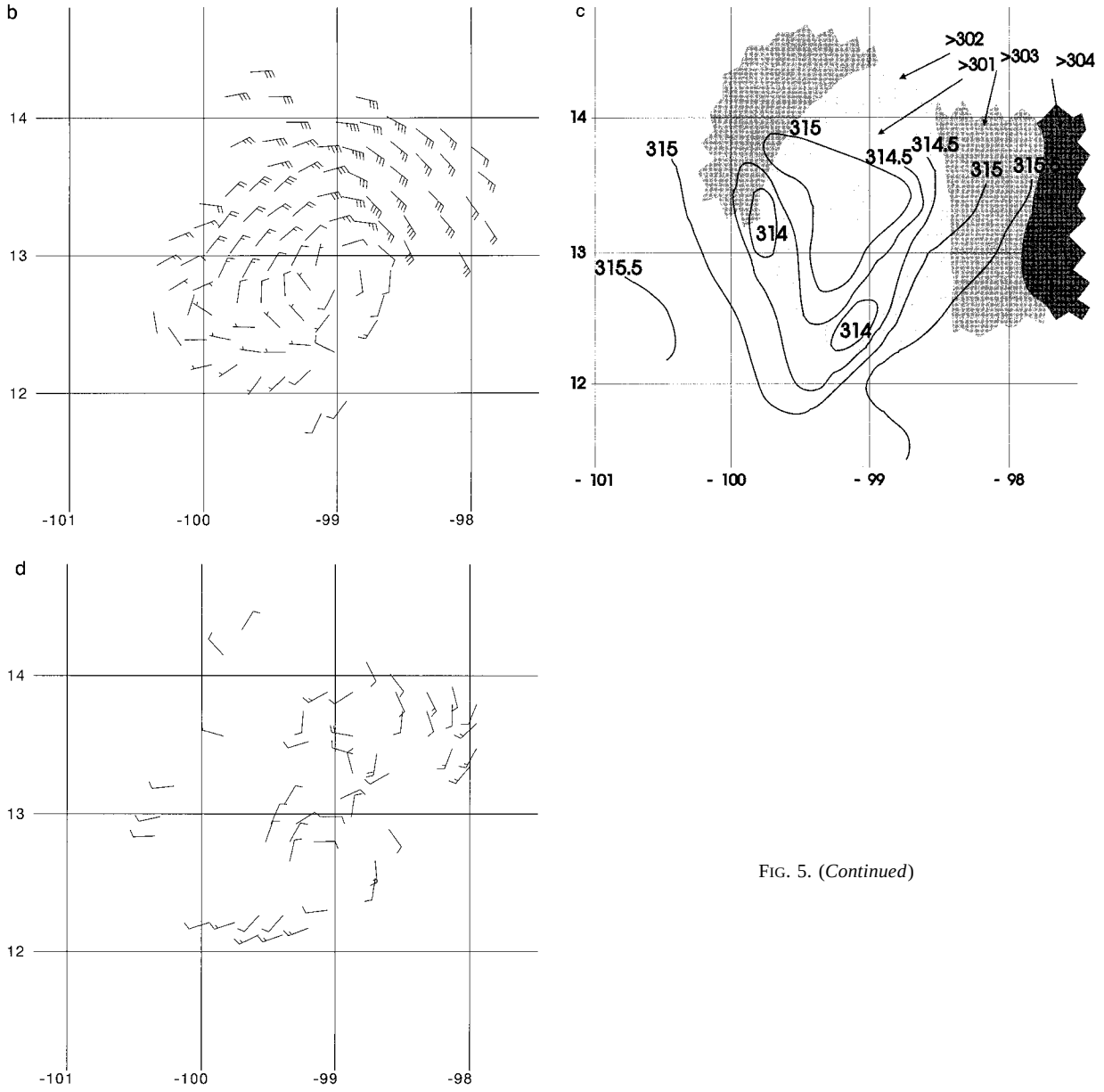

FIG. 5. (*Continued*)

boundary layer and at 3-km altitude while the tangential wind speed increases suggests that intensification owing to the feedback between the wind and the surface heat fluxes is underway.

The main goal of TEXMEX was to test whether elevation of Θ_e in the middle troposphere is a necessary and sufficient condition for tropical cyclogenesis. Analysis of the MCS that developed into Hurricane Guillermo showed a moderate increase of Θ_e at 3-km altitude. The value of Θ_e remained constant for over a day before rapid strengthening of the low-level wind started, suggesting that the observed increase of midtropospheric Θ_e was not enough to start the intensification. The analyzed disturbance was very different from the warm-core disturbance used in the initial state in the simulations on which the TEXMEX hypothesis was based. A vortex, with cyclonic wind increasing with height in the lower troposphere, was found in the stratiform precipitation region of the MCS. The vortex had a cold core in the lower troposphere. At 3-km altitude the relative humidity was anomalously high.[1] There are three problems we try to solve to understand the development of Hurricane Guillermo. First, how did the

[1] Note that high relative humidity is often associated with a positive anomaly in Θ_e. However, in a cold-core system relative humidity can be elevated even if there is no Θ_e anomaly.

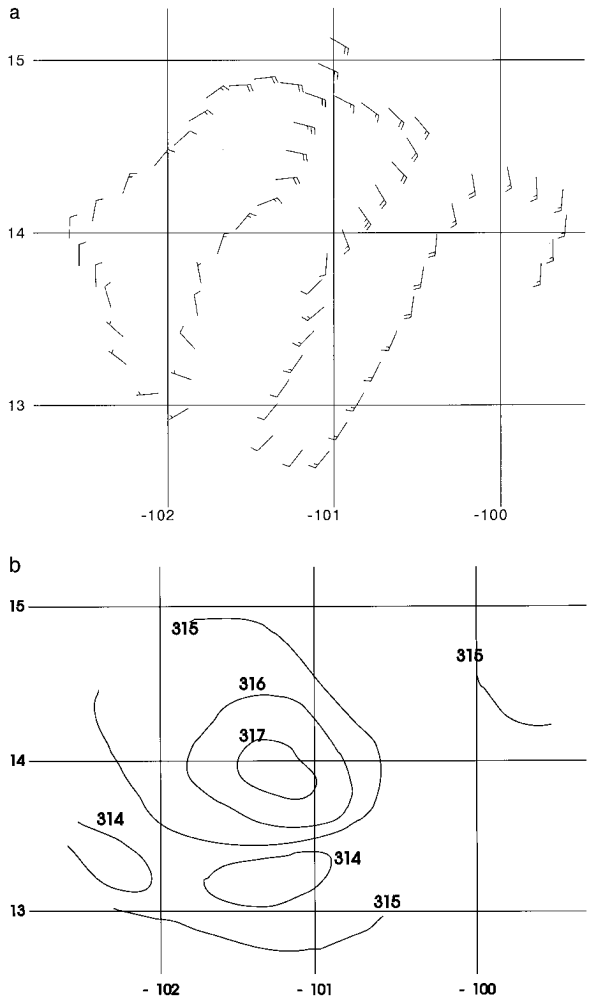

FIG. 6. Tropical Storm Guillermo during flight 5E. (a) In situ wind at 3 km. (b) Virtual potential temperature at 3 km. Units as in Fig. 4.

initial disturbance with a cold-core vortex and high relative humidity form in the stratiform precipitation region of the MCS? Second, is the existence of a cold-core vortex conducive to tropical cyclogenesis? Third, is the cold-core vortex or the high relative humidity more important for cyclogenesis?

Although MCSs are abundant over tropical oceans, only a small minority develops into hurricanes. It is not known why some MCSs are able to develop into tropical cyclones while most are not. Gray (1988) noted that large-scale conditions that favor tropical cyclogenesis include small vertical wind shear and a low-level cyclonic circulation. A correlation of tropical cyclones and the convective phase of the Madden–Julian oscillation (MJO) in the western Pacific was observed by Liebmann et al. (1994).

It has been suggested that upper-tropospheric potential vorticity (PV) anomalies could trigger tropical cyclogenesis. An observational study of tropical cyclogenesis over the western North Pacific (Reilly 1992) indicated that advection of upper-tropospheric PV anomalies often preceded tropical cyclogenesis, while Molinari et al. (1995) noted that the intensification of Hurricane Emily was associated with the approach of an upper-tropospheric PV anomaly. They noted, however, that a weakening of the incipient storm could result from the large vertical shear associated with the upper-tropospheric PV anomaly. This is consistent with the observation that an approaching upper-troposheric trough sometimes seems to cause an incipient storm to die (Simpson and Riehl 1981). Here we note that the ECMWF analyses show no independent upper-tropospheric PV anomalies in the vicinity of the MCS that developed into Hurricane Guillermo (J. Molinari 1996, personal communication).

TABLE 2. Averages of in situ data in a 140 km × 140 km box around the vortex from the two flight altitudes for flights 2P, 4P, and 6P.

	2P	4P	6P
RH (%), 3.0 km	83	85	81
RH (%), 0.3 km	85	92	91
Θ_e (K), 3 km	338	339	345
Θ_e (K), 0.3 km	342	345	350
Θ_v (K), 3 km	315	315	318
Θ_v (K), 0.3 km	302	302	304

The easterly wave and its interaction with topography may have been important factors in increasing vorticity initially, as suggested by FZ. Indeed, tropical cyclogenesis over the eastern Pacific has often been observed to be associated with easterly waves (Miller 1991). It is less clear what relationship exists between easterly waves and MCSs over the eastern Pacific. However, both mesoscale convective complexes (MCC) (Velasco and Fritsch 1987) and tropical cyclones (Zehnder and Gall 1991) are more frequent over the eastern North Pacific than over the Caribbean. There is also ample evidence in satellite imagery of MCCs leading to tropical cyclogenesis (e.g., Velasco and Fritsch 1987; Laing and Fritsch 1993). In addition, there is direct evidence of tropical cyclogenesis from MCSs with a midlevel vortex. Bosart and Sanders (1981) studied one such midlatitude MCS in which a midlevel vortex had developed. The vorticity extended to quite low altitudes, but there was no evidence of a surface circulation before the system moved over the ocean. Observations by Davidson et al. (1990) show that the Australian Monsoon Experiment Tropical Cyclones Irma and Jason initially had maximum intensity in the middle troposphere. These studies and the present case study suggest that the midtropospheric vortex may play an important role in tropical cyclogenesis.

Midtropospheric vortices have been observed in circular MCSs (e.g., Bartels and Maddox 1991) and in squall lines (e.g., Gamache and Houze 1985). It has been suggested that these vortices may result from vertical heating gradients in the stratiform precipitation region. On the other hand, results of numerical simulations of

a squall line by Davis and Weisman (1994) suggest that line-end vortices can form from horizontal heating gradients acting on the initially horizontal vorticity. We have little reason to believe that this mechanism was responsible for the intensification of the vortex in the pre-Guillermo MCS, because the ECMWF wind analysis at 0000 UTC 3 August (Fig. 3) shows that the area where the cyclone was first observed during flight 2P at 0400 UTC 3 August, 10.5°N, 95°W, was characterized by small vertical wind shear below 500 hPa. There may have been shear produced by the line of convection that is the first stage of the MCS; however, the rapid disintegration of this line, as shown in the satellite imagery (Figs. 2a–c), suggests that any shear associated with it was short lived.

The early stage of tropical cyclogenesis from an MCS has been simulated by Chen and Frank (1993). Their initial condition was characterized by a large value of CAPE and a very moist lower troposphere. A midlevel vortex forms owing to the vertical gradient of heating in the anvil and it descends downward in their simulation. They associate the movement of the midlevel vortex downward with the downward development of updraft and warm core in the stratiform rain region. By as early as 8 h of simulated time, the warm-core structure extends down to 850 hPa. This rapid downward extension of the warm core is unlike what was observed in the pre-Guillermo MCS, where it takes about 2 days for the warm core to develop in the lower troposphere. Moreover, analysis of Θ_e from flights 1E and 2P (not shown) indicates that the thermodynamic environment of the MCS at 700 hPa was characterized by a rather dry middle troposphere. It is unlikely that the kind of downward development that occurs in the simulations of Chen and Frank could occur in an environment with a dry middle troposphere.

Based on the data analysis, we postulate the following mechanism for the development of Hurricane Guillermo: An MCS with an extensive stratiform precipitation region forms. Diabatic heating in the upper troposphere and cooling at and below the melting level lead to a formation of a midlevel vortex. Evaporation of rain increases relative humidity in the lower troposphere and leads to a downdraft that advects the vortex downward. Convection redevelops, leading to a further increase of vorticity below the maximum heating and a formation of a warm core.

We anticipate that without the extension of the vortex with its associated lower-tropospheric cold core down into the boundary layer, tropical cyclogenesis is unlikely. Latent heating in the anvil region of an MCS could lead to increased vorticity below the maximum heating and adiabatic cooling below the anvil. On the other hand, the increase of vorticity resulting from diabatic heating in the anvil is not likely to extend down to the boundary layer. Therefore, we expect that the diabatic cooling associated with the evaporation of rain is of paramount importance in transporting the initially midtropospheric vortex down toward the sea surface. While a large-scale stabilization associated with the diabatic heating could result from deep convection in MCSs, they do tend to develop in regions of large-scale ascent (Cotton and Anthes 1989, 594), so it is probable that the deep convective heating is at least partially canceled by the adiabatic cooling associated with large-scale ascent.

These considerations lead us to a hypothesis that cooling by evaporation of mesoscale stratiform precipitation can lead to a lower-tropospheric cold-core vortex that initiates tropical cyclogenesis. We use the axisymmetric model by Rotunno and Emanuel, to be discussed in the next section, to test this hypothesis. We consider the formation of the MCS itself to be beyond the scope of this work; more specifically, we will not try to simulate the development and life cycle of the MCS. Generally, the formation of MCSs may be related to tropical waves, the MJO, sea–land breezes, or independent upper-tropospheric PV anomalies; but in this study, we simply assume the existence of an MCS. We attempt to test a hypothesis that pertains to a particular stage of development of the IOP 5 tropical cyclone; we do not pretend to simulate the entire development.

5. Numerical model

The axisymmetric, nonhydrostatic, convection-resolving model developed by RE is used for the numerical experiments. Some changes were made to the model described in RE: Predictive equations for cloud water and rainwater mixing ratios were added using Kessler microphysics; the horizontal resolution was increased by a factor of 2, and the time step was halved. (Thus the horizontal resolution is 7.5 km, and the time step is 10 s.) The horizontal resolution was increased because of the very small scale of the developing storm when compared to the scale of storms in RE's simulations. The model's outer radius was doubled to 3000 km to avoid spurious effects resulting from partial wave reflection. The upper sponge layer was lifted by 5 km. (The model was not very sensitive to this change, nor to increasing the vertical resolution, so the value of 1250 m used by RE was retained.)

Turbulence restricted to two dimensions is known to cause upscale energy transfer. To minimize this problem, we designed the experiments to minimize the convection in the environment of the disturbance by including no radiation or background wind in any of the simulations.

The initial sounding is the same as that used by RE and is nearly neutral to the model's convection. With the different microphysics scheme, the effective stability of the initial state could be different, but probably not significantly so.

6. Rain shower simulation results

To test the hypothesis that evaporation of steady, mesoscale precipitation could lead to development of a

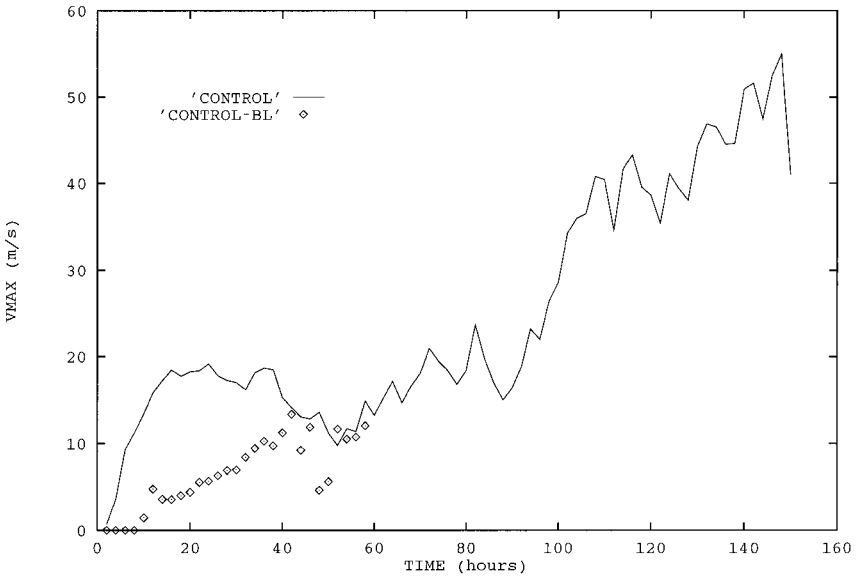

FIG. 7. Maximum tangential wind as a function of time above lowest model level (solid) and at the lowest model level (diamond).

moist vortex with a lower-tropospheric cold core, a simple numerical experiment was designed. A steady mesoscale ''rain shaft,'' emanating from a prescribed altitude, is switched on at the beginning of the simulation. Any latent heating associated with the formation of this rain is neglected.

Neither wind nor virtual temperature perturbations are present in the initial state of the model. However, a positive anomaly in the relative humidity with a maximum value of 80% is prescribed in the upper troposphere, to reflect the high relative humidity of the anvil, from which the precipitation would fall in a real MCS. The temperature is adjusted slightly so that the increase in humidity does not lead to an anomaly in virtual potential temperature. The anomaly in relative humidity is maintained for 36 h. The rainwater mixing ratio is set to 0.1425 g kg^{-1} at 4.375-km altitude during the first 36 h of the simulation. This value is about 25% larger than that deduced from radar observations during flight 2P. The rain shaft extends to 116-km radius, outside of which the imposed flux of rainwater decreases linearly to zero over a radial distance of 37.5 km. The value of the Coriolis parameter at latitude 12°N is used. These values are consistent with observations of the system during flight 2P. The model does not have ice physics. Melting would presumably deepen the layer of diabatic cooling by roughly a kilometer.

a. Control simulation

The development of the maximum tangential velocity in the control run above the lowest model level (625 m) and at the lowest level is shown in Fig. 7. The initial vortex develops rapidly, but at 6 h the tangential wind under the rain shaft is still slightly anticyclonic at the lowest model level. At 16 h the maximum cyclonic wind at the lowest model level is 4 m s^{-1}. There is a positive anomaly of relative humidity above 2.5 km in the region of the rain shaft, extending to the surface within a 20-km radius. The evaporation rate steadily decreases with time in this region. By 24 h, the maximum tangential wind at the lowest model level is 6 m s^{-1}, and some shallow convection has developed about 35 km from the vortex center.

It is perhaps surprising that shallow convection occurs in the middle of the rain shaft. When the rain is turned on, most cooling occurs at the top of the layer containing rain, resulting in cold and moist anomalies above 2 km (Figs. 8a and 8b). Below 2 km, positive temperature and negative relative humidity anomalies result from subsidence forced by the evaporatively driven downdraft above. As the moistening proceeds within the inner 60 km above 2 km, less evaporation of rain occurs there and more rain reaches the lowest 2 km; thus, more evaporation occurs there. The warm and dry pool of air below the rain shaft close to the surface disappears (Figs. 8d and 8e), and by 22 h the cold core extends to the surface within the innermost 90 km (Fig. 8g). The extension of the cold core all the way to the boundary layer explains how shallow convection can develop in the middle of the rain shaft, when there is still a negative Θ_e anomaly of several degrees in the boundary layer. A decrease of temperature by 1 K corresponds to a decrease in saturation Θ_e of 2.5 K for the appropriate temperature values; thus, the evaporation efficiently reduces stability for shallow convection. Sea surface fluxes are also important for the development of the shallow convection; if they are set to zero, the developing shal-

low convection is very weak. It should be noted that, in the model, the sea surface fluxes depend on the perturbation wind field as there is no mean wind.

The flow is divergent in the boundary layer under the rain shaft. Initially, the divergence leads to anticyclonic motion in the boundary layer (Fig. 8c) associated with a mesohigh (not shown); however, vertical advection eventually increases cyclonic wind below the level of convergence (Fig. 8f). By this time, the positive surface pressure anomaly has disappeared from below the center of the vortex (not shown). Between 14 and 22 h the maximum tangential wind speed has changed little; however, the cyclonic wind speed in the boundary layer and the horizontal extent of the cyclone have increased. After shallow convection erupts at 24 h, convergence associated with developing shallow convection further increases the cyclonic wind in the boundary layer, leading to increased sea surface fluxes. Finally, at 48 h, deep convection develops at the 60-km radius. By 60 h, there is deep convection from the 30- to 260-km radius. The deep convection outside the inner 100 km is transient and is associated with downdrafts, while the deep convection within the inner 100 km is more persistent. The largest tangential velocity can be found at the lowest model level starting at 64 h. The vortex is still associated with a lower-tropospheric cold core at this time, but the coldest temperature is no longer at the center. At 96 h there is already a positive potential temperature anomaly in the center at the lowest model level.

The structure of the mature storm is like that in RE, but smaller in size, with hurricane-strength winds extending only to the 30-km radius. The size of the storm is comparable to that of Inez of 1966 (Hawkins and Imbembo 1976).

b. Sensitivity studies

We next discuss the model's sensitivity to several characteristics of the imposed rain shaft. The initial conditions of the sensitivity studies are listed in Table 3. The maximum tangential wind speeds from these sensitivity studies are shown in Figs. 9 and 10.

The value of the rain water mixing ratio of the imposed rain shaft was doubled in DI (''double intensity'') and halved in HI (''half intensity''). After 50 h, the maximum tangential velocity increases in DI, whereas in HI it decreases until 90 h, after which it starts to increase slowly. There are two main differences between the character of the convection in these experiments. First, in DI, deep convection develops between 20 and 30 h, but in HI it takes 100 h. Second, in DI, deep convection first develops at the 450-km radius, and the maximum vertical velocities between 20 and 60 h are generally found at a radius of more than 450 km, whereas in HI deep convection is usually strongest within a few tens of kilometers from the center.

In DI there is more evaporation of rain than in the control simulation. Accordingly, the downdraft and anomalies in temperature and relative humidity are larger. Even though the maximum tangential velocity is not much larger than in the control simulation, the tangential velocity is larger in the boundary layer, and the positive anomaly there extends to larger radius when the showerhead is switched off. Also, the outflow in the boundary layer is stronger than in the control simulation and it occurs at a lower altitude. This results in larger anticyclonic wind, and the larger wind speed close to the sea surface results in increased sea surface fluxes ahead of the outflow of low-Θ_e air. At 32 h, the maximum anomaly of Θ_e in the boundary layer is 5 K in DI and 2 K in the control simulation. The increased sea surface fluxes seem to be the reason for the convection developing at 450 km in DI.

In HI the boundary layer is drier and warmer than in the control simulation at the time at which the showerhead is switched off. The cold core is mainly above the boundary layer, except within the inner 70 km, whereas in the control simulation, the humid cold core extends all the way to the boundary layer. The extension of the humid cold core and outflow to lower altitudes in the control simulation is likely owing to larger evaporation than in HI, especially at lower altitudes.

Sensitivity to the areal coverage of the initial rainshaft was tested by doubling the rain shaft area in DA (''double area'') and halving it in HA (''half area''). By the end of the simulation, the maximum wind speed in DA is about 20 m s^{-1} stronger than in the control simulation, and in HA it is about 20 m s^{-1} weaker. The initial development of the maximum tangential velocity is fairly similar in HA and DA; however, after 80 h the storm in HA becomes quasi-steady and then weakens after 110 h.

The evaporation in DA induces anomalies of wind, temperature, and relative humidity over a larger area, and the wind anomalies are closer to the sea surface than in the control simulation. The outflow extends over a larger range of radii, resulting in larger anticyclonic wind, located closer to the sea surface than in the control simulation. This results in increased sea surface fluxes. As in DI, outer convection develops. Once the outer convection weakens, the storm in the DA simulation starts intensifying. On the other hand, the storm in HA does not suffer from convection occurring in the outer regions, but the inflow of low Θ_e in the lowest 2.5 km causes the rapid weakening of the HA storm at about 110 h. A higher horizontal resolution might be needed to simulate HA properly. On the other hand, the magnitude of the negative anomaly of Θ_e is the same in HA and DA, whereas the wind speed is smaller in HA. This probably explains why Θ_e has not been replenished in HA.

Halving the duration of the rain shaft (experiment HD, ''half duration'') results in slow development of the storm. The tendency of Θ_e at the lowest model level is hardly positive when the showerhead is switched off, apparently owing to small wind speed in the boundary layer (Fig. 8f). It takes 72 h before deep convection

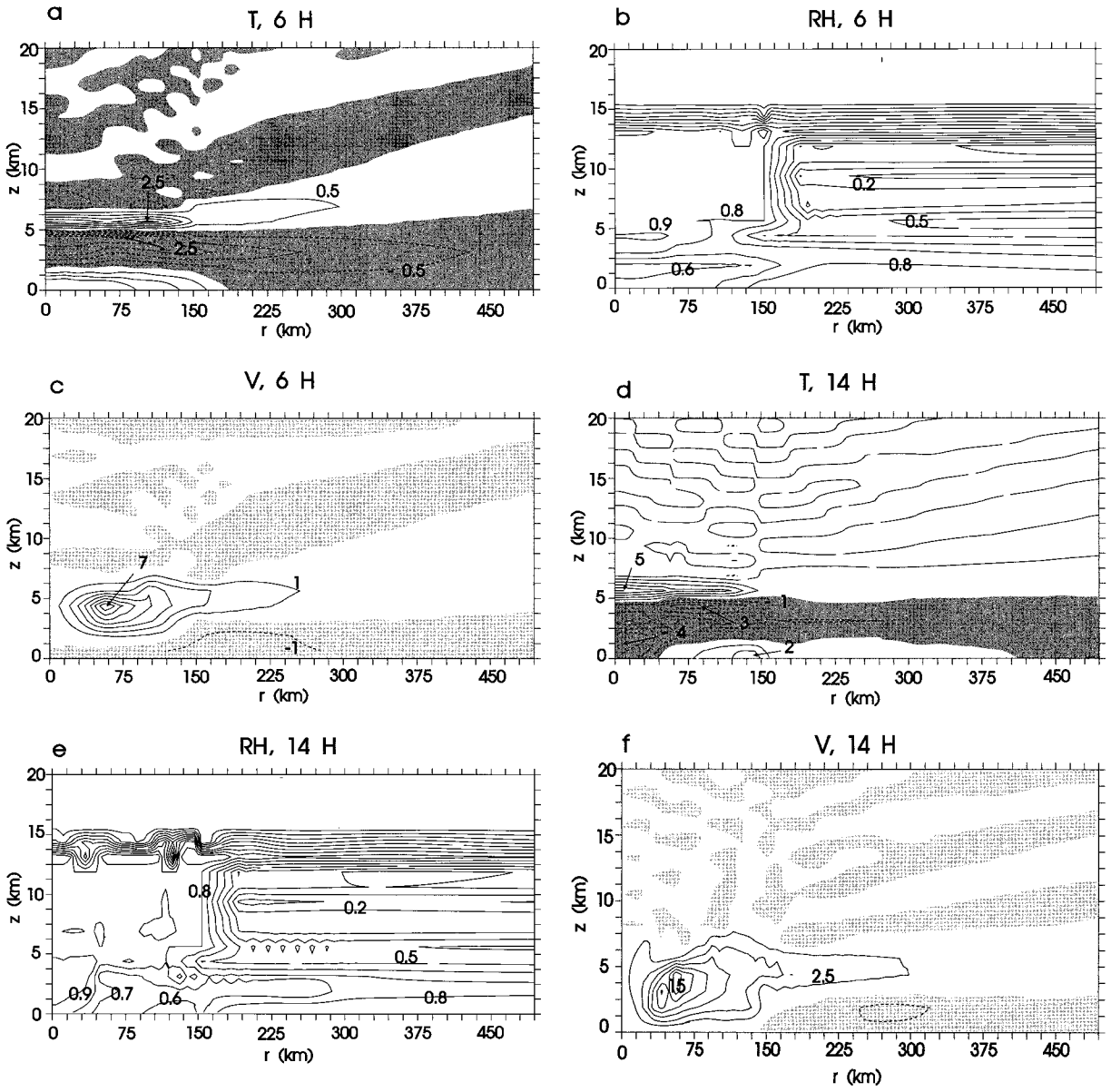

FIG. 8. Average of temperature anomaly (K), relative humidity (%), and tangential velocity (m s^{-1}) in the control simulation between 4 and 8 h (a)–(c), between 12 and 16 h (d)–(f), and between 20 and 24 h in (g)–(i). Negative values stippled.

develops within a radius of 100 km. The weakening at 120 h is associated with low-Θ_e air flowing toward the center in the lower troposphere.

The observed MCS lasted, with variations in the intensity of convection, from the early morning of 2 August 1991 until the vortex reached hurricane strength on 5 August 1991. MCSs usually last less than a day. In experiment HDDI (''half duration–double intensity'') the duration of the rain was halved and the intensity of the rain doubled. The rain intensity was doubled because, judging from satellite imagery, convective activity was at a minimum during flight 2P from which the estimate of the rain rate for the control simulation was obtained. The development of the maximum value of the tangential wind is shown in Fig. 10. As in the control simulation, a warm core develops inside a cold core. The maximum wind reaches 30 m s^{-1} by 80 h. The developing hurricane is qualitatively similar to that of the control simulation; however, deep convection develops 450 km from the center after 20 h. Until the end of the simulation, there is a tendency for convection to develop farther than 150 km from the center, and this convection often exceeds the inner convection in strength.

Based on sensitivity studies DI, DA, and HDDI, it seems that convection in the outer regions can reduce

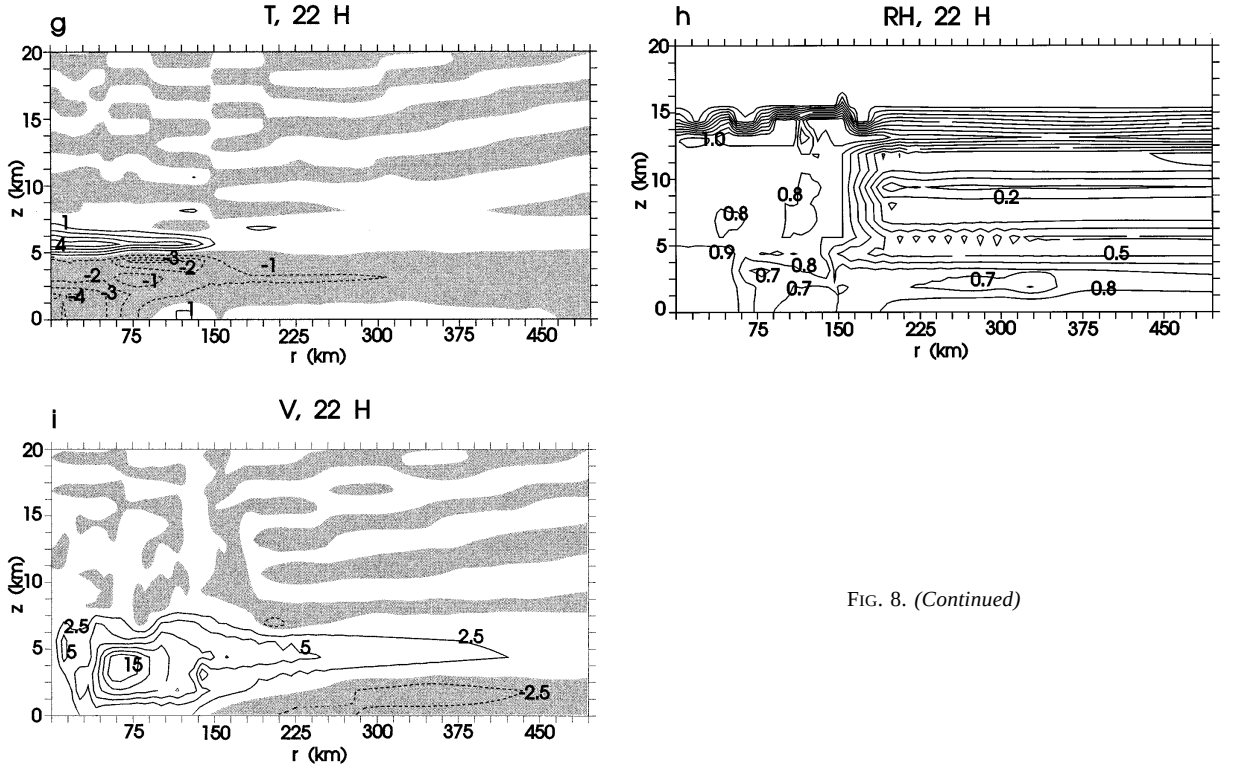

FIG. 8. *(Continued)*

markedly the rate of intensification. The outer convection seems to develop because of increased surface fluxes associated with the outflow and anticyclone at the model's lowest level. To see the effect of the outer convection, HDDI was run anew, but with sea surface fluxes set to zero outside the 340-km radius. No outer convection develops in this experiment. Without the outer convection, a hurricane forms in 3 days and reaches 50 m s^{-1} maximum wind by the end of the simulation (Fig. 10). This shows that the effect of the outer convection is clearly detrimental. The strength of the outer convection may be at least partially an artifact of the absence of a mean background wind and radiation in the model. A mean wind of 3 m s^{-1} would probably be appropriate for a typical tropical boundary layer. If a radial or tangential wind velocity of 3 m s^{-1} is added to the mean wind, the azimuthally averaged wind speed is 3.8 m s^{-1}, only 27% larger than the mean wind speed. This would not increase the sea surface fluxes as much as would the increase of the wind speed from 0 to 3 m s^{-1}.

TABLE 3. Model simulations: q is mixing ratio of showerhead (g kg^{-1}), r is radius of showerhead (km), and Δt is duration of showerhead (h).

Experiment	How differs from control
CONTROL	—
DI	$q = 0.2850$ (rain mixing ratio doubled)
HI	$q = 0.07125$ (rain mixing ratio halved)
DA	$r = 188$ (area doubled)
HA	$r = 98$ (area halved)
HD	$\Delta t = 18$ (duration halved)
HDDI	$\Delta t = 18$, $q = 0.2850$
HDDI-FLUX	Same as HDDI but no surface fluxes for $r > 340$ km

A set of experiments was run to study the effect of the *initial value* of the middle-tropospheric relative humidity (Bister 1996). The initial middle-tropospheric relative humidity was increased by 30% in one experiment and it was decreased by 30% in another experiment. The results show that a dry middle troposphere favors the initial development of the cold-core vortex. However, a moist middle troposphere is slightly more favorable at later stages of the development. The overall development is not sensitive to the large-scale humidity in the middle troposphere. This is consistent with the observation by McBride and Zehr (1981), showing that midtropospheric relative humidities do not differ in the large-scale environments of cloud clusters that intensify into hurricanes and those that do not.

c. Comparison of the observations and the simulation

The analysis of the pre-Guillermo system and the control simulation show many similarities. First, it takes about the same time (3–4 days) for the system to develop into a hurricane from the start of mesoscale precipitation. The model simulation shows the development of a cold-core vortex with high relative humidity in the core of the imposed rain shaft. A cold-core vortex with high relative humidity was observed in the stratiform

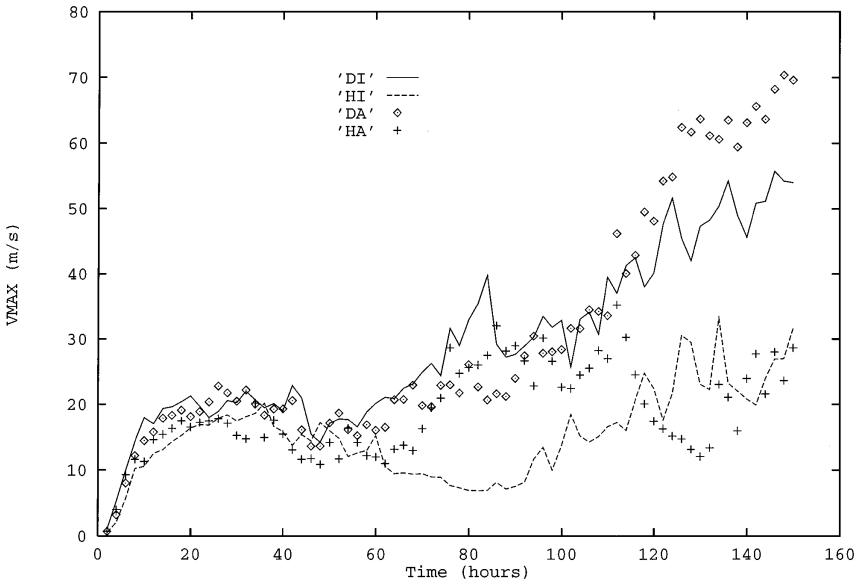

FIG. 9. Maximum tangential velocity as a function of time in experiments DI (solid), HI (dashed), DA (diamond), and HA (plus).

precipitation region on flight 2P. Between the end of the imposed rain shaft in the model at 36 h and the rapid intensification that starts after 90 h, a warm core develops within the lower-tropospheric cold core. The value of Θ_e has increased by 4–5 K at the lowest level inside the 150-km radius. Both the replacement of the cold core by a warm core inside a weakened cold core and the increase of Θ_e in the boundary layer by several degrees were also observed to occur in the pre-Guillermo system between flights 2P and 4P.

It takes about 50 h for deep convection to develop in the control simulation. On the contrary, satellite images do not show as long a time interval without cold cloud tops in the region of the MCS. This discrepancy might result from the lack of a mean wind in the model experiments. Easterly mean wind adds to the vortex wind on the northern side and would tend to favor convection there. The observations indeed show that convection is preferred on the northern side of the vortex center.

7. The roles of cold-core vortices and relative humidity in cyclogenesis

Both in reality and in the control simulation a tropical cyclone develops from a state with a lower-tropospheric cold-core vortex and high relative humidity. To assess the relative importance of the high humidity and the cold-core vortex, three simulations, B1, B2, and B3, were run with simple initial disturbances (Table 4).

In experiment B2 there is no wind in the initial condition, but the relative humidity is set to 100%, keeping virtual potential temperature constant, in a cylinder of 68 km in radius and extending from 2.5 to 12.5 km in altitude. In experiment B1 a cold-core vortex was added to the initial state of experiment B2. The vortex has a maximum tangential velocity of 9 m s^{-1} at the 3.1-km altitude. The maximum tangential velocity is reached at a radius of 64 km from the center, and the velocity vanishes at a radius of 338 km. The radial profile is the same as in RE. The velocity increases linearly with height up to 3.1 km, and above it decreases linearly to zero at the base of the sponge layer.[2] Temperature is decreased in the region with 100% relative humidity so as to conserve virtual potential temperature. In experiment B3 the same vortex is used as in experiment B1, but the mixing ratio of water vapor is horizontally homogeneous. The associated anomalies of Θ_e and relative humidity are small. In experiments B1 and B2 the anomalies of Θ_e in the middle troposphere are close to those observed on flight 2P. In all these experiments the wind velocity in the drag law was set to have a minimum value of 3 m s^{-1} in the calculation of heat fluxes within 112.5-km radius. In these simulations, the outer radius of the model was set to 1500 km, half of that used in all of the other simulations.

The maximum tangential velocities in B1, B2, and B3 are shown in Fig. 11. In experiment B2 convection develops within hours, but inflow above the boundary layer decreases relative humidity and downdrafts develop. The value of Θ_e decreases greatly in the boundary

[2] The wind associated with the initial cold-core cyclone in B1 and B3 was made to decrease to zero at the bottom of the sponge layer, which lies at the 24-km altitude. Another set of simulations in which the cyclonic winds were made to decrease to zero at 17 km showed qualitatively similar results.

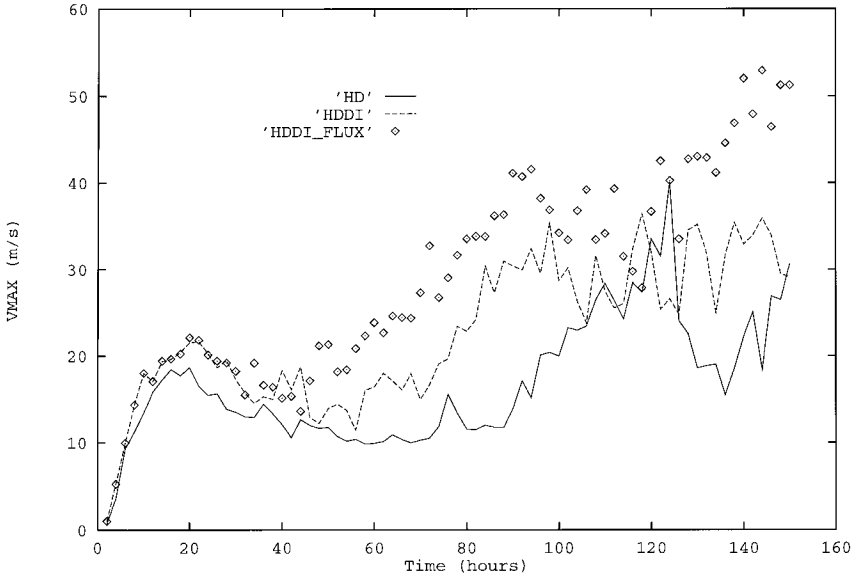

FIG. 10. Maximum tangential velocity as a function of time in experiments HD (solid), HDDI (dashed), and HDDI with surface fluxes set to 0 outside 340 km (diamond).

layer, suppressing convection. The system fails to intensify by 150 h. This contradicts simulation results of Emanuel (1995) showing that saturation of a mesoscale column is a sufficient condition for cyclogenesis. The discrepancy probably results from the different scale of the initial moist column. In experiment B2 it is 68 km in radius, while in Emanuel's study it is 150 km in radius. It should be noted that the moist column, with relative humidity exceeding 90%, in the observations (Fig. 4) is about 50 km in radius, and in the control simulation the area covered by 90% relative humidity extends to 70 km in radius when the showerhead is switched off. Experiment B2 was run anew but with the moist column extending to 150 km. By the end of this simulation, the system is a marginal hurricane, confirming Emanuel's result that *a broad enough* column of saturated air by itself can result in a hurricane.

In experiment B1 convection also develops within hours. There is initially as much cooling by evaporation in the two simulations. However, convection does not cease in B1. There are two possible reasons for this. First, at 16 h, Θ_e is small in both experiments, but experiment B1 shows conditional instability because the cold anomaly of about 3 K in the lowest few kilometers implies a negative anomaly of saturation Θ_e of about 8 K. Second, in B2, there is strong inflow at midlevels, feeding convection. This inflow extends all the way to the inner core of the system. There is no such strong inflow in experiment B1, perhaps owing to increased inertial stability.

TABLE 4. Idealized initial conditions in simulations that address the roles of cold-core vortices and relative humidity.

Experiment	Initial conditions
B1	Midlevel vortex and high relative humidity
B2	High relative humidity only
B3	Midlevel vortex only

Experiment B3 shows that without the high relative humidity development of the initial cold core into a hurricane is delayed by 2 days, because of larger evaporation of rain and cloud, and stronger downdrafts. Even though the downdraft air in experiment B3 has smaller Θ_e than in experiment B2, the disturbance in experiment B3 develops more rapidly than in experiment B2. Therefore, it does not seem to be the case that the favorable effect of the initial cold-core vortex is owing to reduction of the inflow of low-Θ_e air by the enhanced inertial stability. The fact that B3 develops 2 days later than B1 suggests that in the presence of a cold-core vortex the initial dryness of the middle troposphere can only delay the system from intensifying.

8. Discussion

The numerical experiments discussed in section 6 were intended to explore the formation of a cold-core mesoscale cyclone by evaporation of mesoscale precipitation from a preexisting MCS. We neglected the effects of deep convection associated with the *initial* MCS in the model simulation. Deep convection would result in an additional flux of low Θ_e into the boundary layer. On the other hand, we did not include a background wind, which would increase the fluxes of heat and moisture from the sea surface.

The rain shaft in the control simulation extends to 116 km in radius and the imposed rain flux then declines linearly to zero over 37.5 km. It is interesting to note

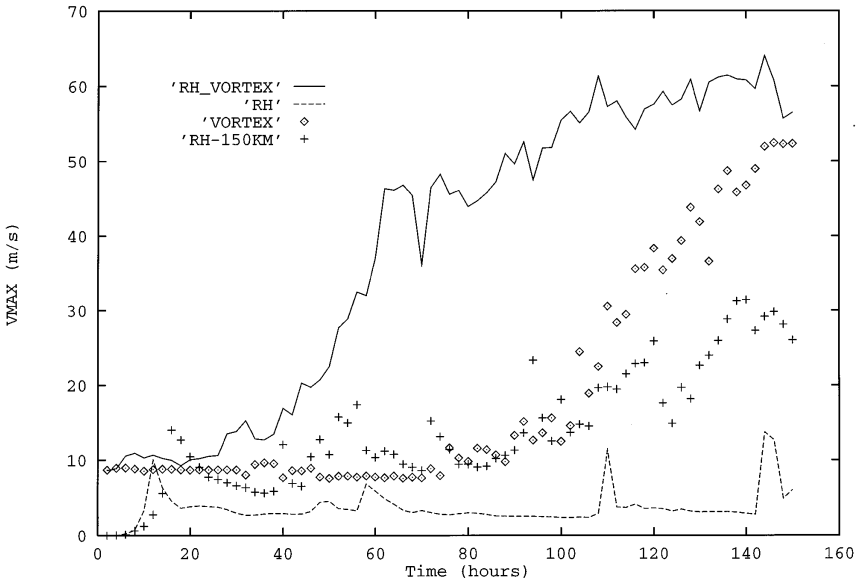

FIG. 11. Maximum tangential velocity in experiments B1 (solid), B2 (dashed), B3 (diamond), and in experiment with moist column extending to 150 km (plus).

that over the western tropical Pacific, 1% of the cloud systems whose areas are defined by the 208-K infrared temperature threshold have been observed to exceed 50 000 km^2 in size, corresponding to 126 km in radius (Houze 1993, 337). The 208-K threshold is often used for correlating infrared temperatures with precipitation. Houze (1993) notes that these large cloud systems account for almost 40% of the total area covered by clouds with this temperature threshold.

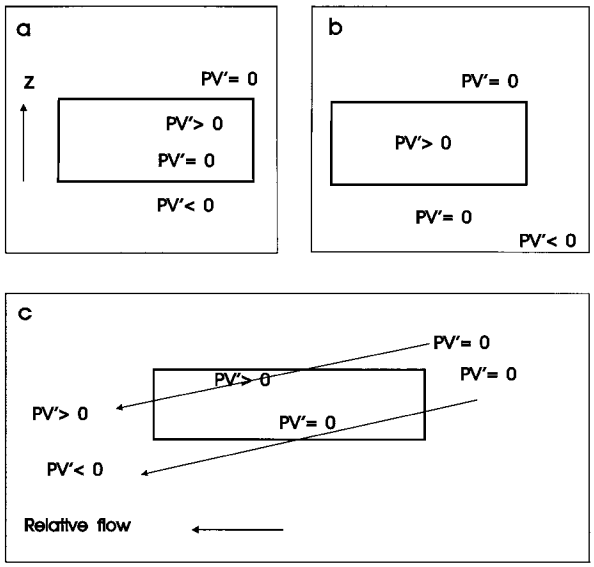

FIG. 12. Thought experiment of cooling in a box. PV anomalies (a) after parcels of air descended half of the depth of the box, (b) after parcels of air descended the depth of the box, and (c) with relative flow, arrows show hypothetical trajectories. In (a) and (b) PV anomalies are symmetric about vertical axis of the box.

The simulations of sections 6 and 7 suggest that a mesoscale cold-core vortex is an ideal embryo for tropical cyclogenesis, provided it eventually extends downward into the boundary layer. If the cold-core vortex does not extend to the boundary layer by the time the rain shaft is switched off, a cyclone develops very slowly, if at all (simulation HD). The vortex winds are important for sea surface fluxes, and the cold core right above the surface enhances convection and diminishes the role of downdrafts in preventing further convection. Therefore, the downward development of the vortex and the associated cold core as a direct result of evaporation (maybe also melting and water loading in practice) may be of crucial importance to tropical cyclogenesis. In this section we offer a few speculations for how the downward development of the vortex may occur, based on a simple thought experiment. We also suggest what processes might prevent the downward development.

Assume that the horizontal component of (relative) vorticity is zero and that the vertical component is constant. Let us switch on constant diabatic cooling in a mesoscale region, depicted in Fig. 12a. Once constant cooling is switched on, air that goes through the upper boundary of cooling experiences an increase of PV of some amount. Air that goes through the lower boundary experiences a decrease of the same amount. Soon there will be a positive PV anomaly within the region of cooling, and a negative PV anomaly below it. When the air that went through the upper boundary of cooling reaches the lower boundary, it will lose its positive PV anomaly and emerge with no anomaly (this applies to the linear case). The initial negative anomaly gets dispersed with divergence below the cylinder (Fig. 12b). In the vorticity field, one would expect a cyclone to

dominate the field below the diabatic cooling. The time it takes for the first parcel of air that went through the upper boundary to reach the lower boundary can be used as a rough estimate for the time it takes for the negative PV anomaly to disappear from directly below the layer of cooling. For a depth of the layer of 4000 m, and vertical velocity of 0.1 m s^{-1}, the timescale is 10 h.

We noted before that in the control simulation, the relative humidity increases in the layer between 2 and 4 km, and this results in more precipitation and thus an enhancement of evaporation within the lowest 2 km. In terms of the thought experiment, the cylinder of cooling descends to lower altitudes. In the control simulation, this occurs in the same time that it takes air to descend 4 km. Both the dispersion of the negative PV anomaly while the positive anomaly is confined to the cylinder and the downward movement of the cylinder of cooling are expected to affect the downward development of the vortex. Note that if the rain rate is increased, the cylinder of cooling is deeper to start with, and air travels faster to the lower boundary of cooling; thus, the downward development of the cyclone can be expected to occur sooner. This is consistent with the results from experiment DI.

Apart from the strength and duration of rain that may be important for the downward development, a relative flow through the system (e.g., owing to environmental shear) could also be important. A scenario with a relative flow is shown in Fig. 12c. That air that goes through the upper boundary of cooling but not through the lower boundary will retain its positive PV anomaly. Air that goes through the lower boundary but not through the upper boundary will retain its negative PV anomaly. Note that in this case the positive (and negative) PV anomaly will be diffuse. Thus vorticity will not increase within the volume of cooling as much as it would without the relative flow through the system. This will make further changes of PV smaller, since diabatic PV production is proportional to vorticity. In this case one would expect to see a weak cyclone above a weak anticyclone. Note that a relative flow through the prepitating system may not only be owing to shear. For example, in a propagating atmospheric wave there is relative flow through the wave even without shear.

It is remarkable that even though squall lines have been observed to produce midlevel cyclones, there are no instances known to the authors of tropical cyclogenesis from squall-line-produced midlevel cyclones. We suggest that this may be owing to two factors. First, the time it takes for air to descend through the layer of stratiform precipitation may be longer than the duration of the stratiform rain in squall lines. This might be due to the short duration of precipitation and/or weak precipitation leading to weak downdrafts. It is interesting that Gamache and Houze's (1985) analysis of a tropical squall line indeed shows that a cyclone resides in the middle troposphere with negative relative vorticity below. Second, a relative flow through the system may explain why, in many squall lines, the midlevel cyclone may be weak if it exists at all.

We summarize the mechanism for tropical cyclogenesis outlined in this work in Fig. 13. First, a long-lasting MCS forms. Evaporative cooling (and anvil heating) results in a midlevel vortex with an upper-tropospheric warm core and lower-tropospheric cold core. Initially, the lower-tropospheric cold core lies above a layer of warm and dry air that is a result of forced subsidence (Fig. 13a). As the system evolves, the vortex extends to lower altitudes, and the cold anomaly expands downward to occupy the whole lower troposphere (Fig. 13b). The extension of the cold-core vortex into the boundary layer favors redevelopment of convection at least in two ways. First, the vortex wind enhances sea surface fluxes. Second, the cold core aloft reduces the value of boundary layer Θ_e that is needed for convection to occur. The redeveloping convection with latent heating further increases vorticity near the surface, resulting in higher wind speed (Fig. 13c). High relative humidity diminishes evaporation of rain and thus discourages convective downdrafts. The evaporative downdraft that does occur is less fatal than it would be for a warm-core cyclone.[3] The formation of a lower-tropospheric humid cold-core vortex that extends to the boundary layer is a way to avoid the downdraft problem that plagues a warm-core disturbance in an otherwise undisturbed environment.

There is some observational evidence of the importance of the cold-core structure extending down to the boundary layer. Zehr (1976) used radiosonde data to study western Pacific cloud clusters, some of which developed into hurricanes. Thermal anomalies in the developing and nondeveloping clusters are shown in Fig. 14. It is remarkable that in nondeveloping clusters the cold core, best defined between 600 and 700 hPa, almost changes to a warm core at 800–900 hPa. This temperature structure resembles the temperature structure in the control simulation at 6 h (Fig. 8a). On the other hand, the cold core extends all the way to the top of the boundary layer in the developing clusters. (The extension of the warm core to a lower altitude than in the nondeveloping clusters may be due to the former's more advanced stage of development.) The difference of temperature between 0°–1° and 0°–3° in the developing clusters suggests a reversal of the temperature gradient within the inner 3°, with a warm core inside a cold core. Indeed, this is also true of the pre-Guillermo system during flight 4P (Figs. 5c and 5d) and the control simulation after 96 h of simulation time.

Raymond and Jiang (1990) proposed another mechanism for the regeneration of convection in MCSs: In

[3] If in an undisturbed tropical atmosphere convection can occur with a boundary layer Θ_e value of 355, then a value of 347 (363) is needed in a cold- (warm-) core cyclone with a 3-K temperature anomaly.

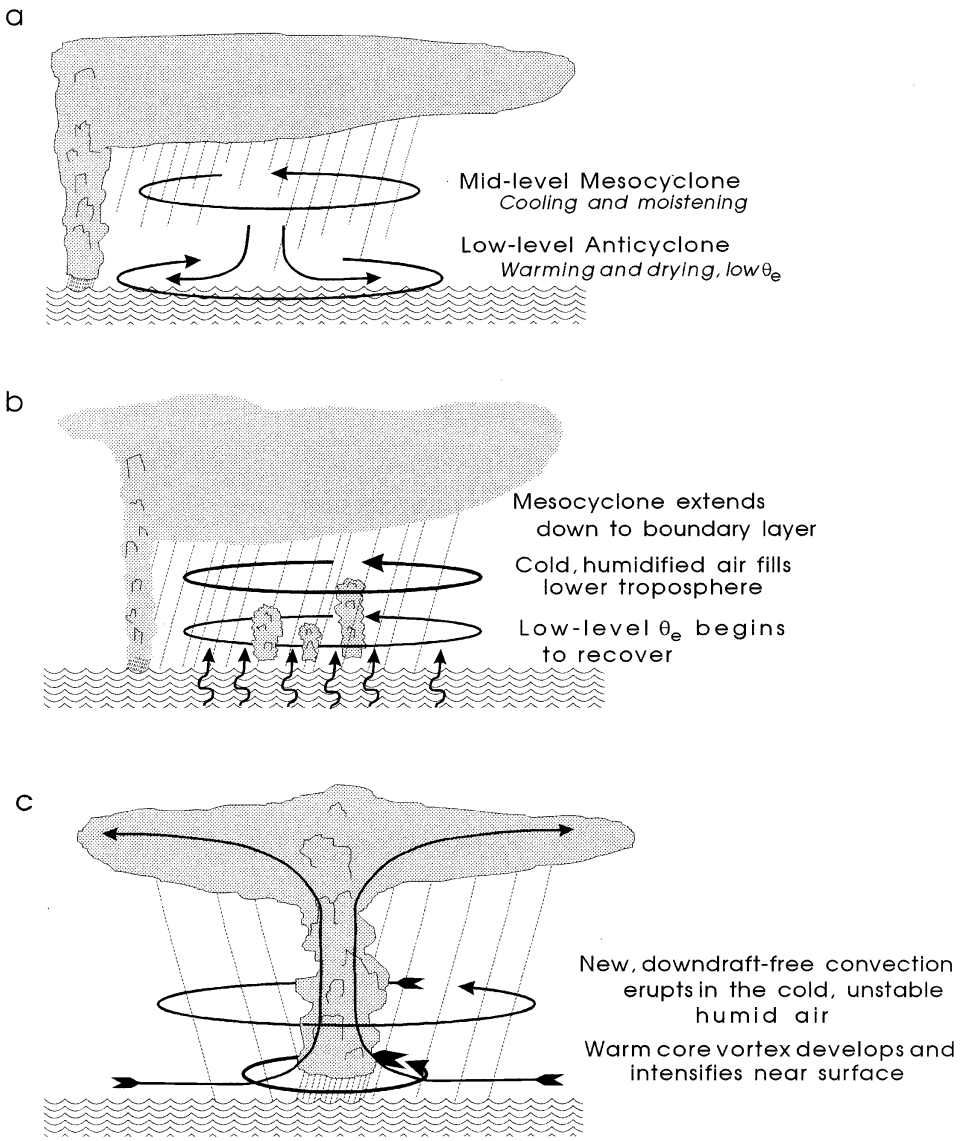

FIG. 13. Conceptual model of tropical cyclogenesis from a preexisting MCS. (a) Evaporation of stratiform precipitation cools and moistens the upper part of the lower troposphere; forced subsidence leads to warming and drying of the lower part. (b) After several hours there is a cold and relatively moist anomaly in the whole lower troposphere. (c) After some recovery of the boundary layer Θ_e convection redevelops. See text for details.

the presence of a midlevel PV anomaly and vertical wind shear between the PV anomaly and lower levels, air below the PV anomaly that flows toward the PV anomaly has to ascend. It is important to note that this mechanism depends on both the shear and a PV anomaly that is confined to the middle troposphere. Fritsch et al. (1994, hereinafter FMK), in an observational study, found evidence for this mechanism operating in a mid-latitude MCS and suggested that the same mechanism might operate in the Tropics, leading to tropical cyclogenesis. However, in their case study a surface mesohigh attended the midlevel vortex throughout its lifetime of several days. We suggest that the surface mesohigh may be attributable to the shear in the way depicted in Fig. 12c. Indeed, FMK note that although the midlevel shear was weak, there was a low-level jet implying larger shear at low altitudes. The observation of a persistent mesohigh should be contrasted with observations from Guillermo showing that even during flight 2P there was a negative pressure anomaly below the center of the vortex at 300 m and with our control simulation showing that by 14 h of simulation time the positive pressure anomaly had disappeared from the surface just below the center of the vortex.

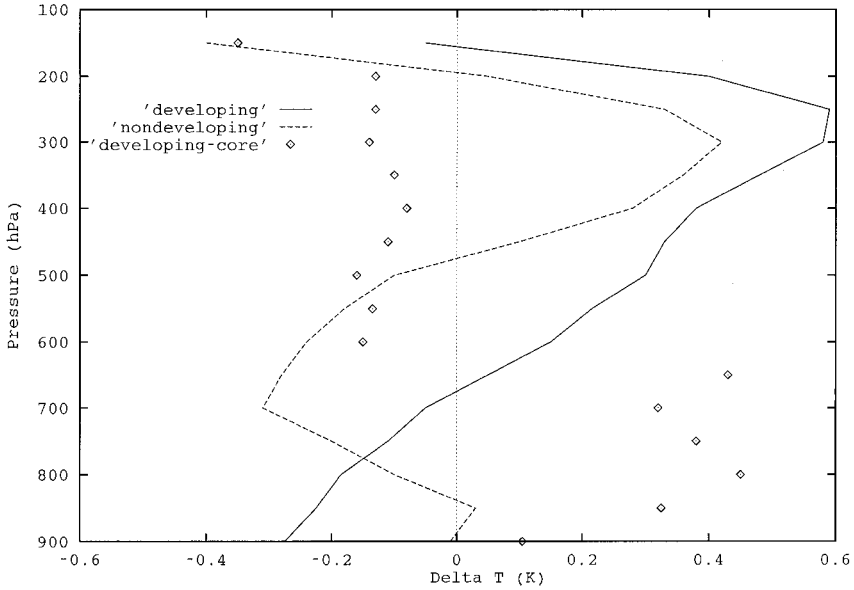

FIG. 14. Thermal anomalies in cloud clusters over western North Pacific. Difference between the temperature within the inner 3° and the environment in developing cloud clusters (solid) and nondeveloping cloud clusters (dashed), and difference between the temperature within the inner 1° and inner 3° in developing clusters (diamonds). The environment is defined here as the 5°–7° band around the center of the cluster. Values taken from Figs. 17 and 20 in Zehr (1976).

9. Conclusions

A mesoscale vortex is initially found in the stratiform precipitation region of a mesoscale convective system that eventually became Hurricane Guillermo. This vortex is relatively cold and humid at the 3-km altitude. Roughly 1 day later, we find at both 3 km and in the boundary layer a small-scale positive anomaly of virtual potential temperature, inside the negative anomaly, and collocated with convection. By flight 5E, 14 h later, the wind speed has increased, and the system has a lower-tropospheric warm core.

Numerical simulations with an axisymmetric model show that prescribed precipitation lasting sufficiently long and covering enough area results in a humid vortex with a lower-tropospheric cold core. The model develops a hurricane in 3 days. Decreasing the rain rate or the duration of the rain results in markedly slower development. If precipitation lasts for only 18 h, but is doubled in strength, a hurricane results, but it is less strong than in the control case, owing to the development of convection several hundred kilometers from the center. (It is not possible to say whether the outer convection would develop were the radiation and the background wind taken into account.)

Mesoscale stratiform precipitation usually does not last for 18–36 h. However, Houze (1993, 337; see also Williams and Houze 1987) notes that some larger MCSs can last as long as 2–3 days. While few MCSs last longer than 1 day, it is also true that only a small percentage of MCSs develop into hurricanes.

Numerical experiments with idealized initial disturbances show that the existence of the initial cold-core vortex is crucial to the further development of the system. High relative humidity hastens the development by 2 days by discouraging convective downdrafts. However, the existence of a *midlevel* vortex is not enough. A sensitivity study in which the duration of the rainshower is halved suggests that cyclogenesis can be prevented if the vortex and the associated lower-tropospheric cold core do not extend down to the boundary.

A simple thought experiment suggests that the downward extension of a cyclonic vortex takes as long as it takes air to descend through the layer with evaporational cooling. For a 4-km-deep layer and a 0.1 m s^{-1} descent velocity, this timescale is 10 h. However, in the control experiment, most of the evaporational cooling initially occurs well above the boundary layer. It takes several hours before the layer from 2 to 4 km moistens so that precipitation, and hence evaporation rates, increases at lower altitudes. The thought experiment also suggests that relative flow through the system could prevent development and/or downward extension of a cyclone. It would seem that to get the needed vortex and its downward extension three things are important. First, precipitation has to last longer than it takes air to descend through the layer of evaporation, to allow for the dispersion of the negative PV anomaly so that the positive anomaly dominates in the rain region. Second, in case of weak precipitation, the upper part of the lower troposphere has to be moistened so that the evaporation rates can increase closer to the surface. Third, relative flow through the system should be small. These three

factors would also favor a more humid vortex core, which in turn is favorable for cyclogenesis.

Simulations with a three-dimensional model are needed to learn more about both the effect of the relative flow through the system on the vortex formation and its downward extension and the effect of the mean flow on surface fluxes and outer convection. Detailed observations from other cases of tropical cyclogenesis are needed to assess whether the downward extension of the cold-core vortex is a necessary condition for the development of the warm-core vortex, as suggested by this study.

Acknowledgments. For their outstanding support of the TEXMEX field operations and postexperiment data handling we are indebted to the staffs of the National Oceanographic and Atmospheric Administrations's Office of Aircraft Operations and to the Research Aviation Facility of the National Center for Atmospheric Research. TEXMEX would not have been possible without the excellent forecast guidance and flight planning provided by staff members of NOAA's National Hurricane Center and Hurricane Research Division (HRD). We are particularly indebted to Stan Rosenthal and Bob Burpee for their generous support of TEXMEX from its inception. We extend special thanks to Odón Sánchez for making everything work and to Señor Lalo McKissack and the staff of the Playa Hermosa for the wonderful hospitality they extended to us during our stay in Acapulco. MB is grateful for the opportunity to edit the Doppler data at HRD using their ready computer programs. Frank Marks's and John Gamache's help was crucial. We also thank Richard Rotunno for providing the numerical model and assisting with its modification and use. This research was supported by the National Science Foundation through Grants ATM 8815008 and ATM 9216906.

REFERENCES

Bargen, D. W., and R. C. Brown, 1980: Interactive radar velocity unfolding. Preprints, *19th Conf. on Radar Meteorology,* Miami Beach, FL, Amer. Meteor. Soc., 278–283.

Bartels, D. L., and R. A. Maddox, 1991: Midlevel cyclonic vortices generated by mesoscale convective systems. *Mon. Wea. Rev.,* **119,** 104–118.

Bister, M., 1996: Development of tropical cyclones from mesoscale convective systems. Ph.D. thesis, Massachusetts Institute of Technology, 112 pp. [Available from Marja Bister, Finnish Meteorological Institute, P.O. Box 503, 00101 Helsinki, Finland.]

Bosart, L. F., and F. Sanders, 1981: The Johnstown flood of July 1977: A long-lived convective system. *J. Atmos. Sci.,* **38,** 1616–1642.

Chen, S. S., and W. M. Frank, 1993: A numerical study of the genesis of extratropical convective mesovortices. Part I: Evolution and dynamics. *J. Atmos. Sci.,* **50,** 2401–2426.

Cotton, W. C., and R. A. Anthes, 1989: *Storm and Cloud Dynamics.* Academic Press, 880 pp.

Davidson, N. E., G. J. Holland, J. L. McBride, and T. D. Keenan, 1990: On the formation of AMEX cyclones Irma and Jason. *Mon. Wea. Rev.,* **118,** 1981–2000.

Davis, C. A., and M. L. Weisman, 1994: Balanced dynamics of mesoscale vortices produced in simulated convective systems. *J. Atmos. Sci.,* **51,** 2005–2030.

Elsberry, R. L., W. M. Frank, G. J. Holland, J. D. Jarrell, and R. L. Southern, 1987: *A Global View of Tropical Cyclones.* University of Chicago Press, 185 pp.

Emanuel, K. A., 1989: The finite-amplitude nature of tropical cyclogenesis. *J. Atmos. Sci.,* **46,** 3431–3456.

——, 1995: The behavior of a simple hurricane model using a convective scheme based on subcloud-layer entropy equilibrium. *J. Atmos. Sci.,* **52,** 3960–3968.

Farfán, L. M., and J. A. Zehnder, 1997: Orographic influence on the synoptic-scale circulations associated with the genesis of Hurricane Guillermo (1991). *Mon. Wea. Rev.,* **125,** 2683–2698.

Fritsch, J. M., J. D. Murphy, and J. S. Kain, 1994: Warm core vortex amplification over land. *J. Atmos. Sci.,* **51,** 1780–1807.

Gamache, J. F., and R. A. Houze Jr., 1985: Further analysis of the composite wind and thermodynamic structure of the 12 September GATE squall line. *Mon. Wea. Rev.,* **113,** 1241–1259.

——, F. D. Marks Jr., and F. Roux, 1995: Comparison of three airborne Doppler sampling techniques with airborne in situ wind observations in Hurricane Gustav (1990). *J. Atmos. Oceanic Technol.,* **12,** 171–181.

Gray, W. M., 1988: Environmental influences on tropical cyclones. *Aust. Meteor. Mag.,* **36,** 127–139.

Hawkins, H. F., and S. M. Imbembo, 1976: The structure of a small, intense hurricane, Inez 1966. *Mon. Wea. Rev.,* **104,** 418–442.

Houze, R. A., Jr., 1993: *Cloud Dynamics.* Academic Press, 573 pp.

Laing, A. G., and J. M. Fritsch, 1993: Mesoscale convective complexes in Africa. *Mon. Wea. Rev.,* **121,** 2254–2263.

Liebmann, B., H. H. Hendon, and J. D. Glick, 1994: The relationship between tropical cyclones of the western Pacific and Indian Oceans and the Madden–Julian oscillation. *J. Meteor. Soc. Japan,* **72,** 401–411.

Marks, F. D., and R. A. Houze, 1987: Inner core structure of Hurricane Alicia from airborne Doppler radar observations. *J. Atmos. Sci.,* **44,** 1296–1317.

McBride, J. L., and R. Zehr, 1981: Observational analysis of tropical cyclone formation. Part II: Comparison of non-developing versus developing systems. *J. Atmos. Sci.,* **38,** 1132–1151.

Miller, R. J., 1991: Tropical cyclogenesis in the eastern North Pacific from an African wave. Preprints, *19th Conf. on Hurricanes and Tropical Meteorology,* Miami, FL, Amer. Meteor. Soc., 245–248.

Molinari, J. S., S. Skubis, and D. Vollaro, 1995: External influences on hurricane intensity. Part III: Potential vorticity structure. *J. Atmos. Sci.,* **52,** 3593–3606.

——, D. Knight, M. Dickinson, D. Vollaro, and S. Skubis, 1997: Potential vorticity, easterly waves, and eastern Pacific tropical cyclogenesis. *Mon. Wea. Rev.,* **125,** 2699–2708.

Raymond, D. J., and H. Jiang, 1990: A theory for long-lived mesoscale convective systems. *J. Atmos. Sci.,* **47,** 3067–3077.

Reilly, D. H., 1992: On the role of upper-tropospheric potential vorticity advection in tropical cyclone formation: Case studies from 1991. M.S. thesis, Dept. of Earth, Atmospheric and Planetary Sciences, Massachusetts Institute of Technology, 124 pp. [Available from Massachusetts Institute of Technology, Room 14-0551, 77 Massachusetts Avenue, Cambridge, MA 02139.]

Rotunno, R., and K. A. Emanuel, 1987: An air–sea interaction theory for tropical cyclones. Part II: Evolutionary study using a nonhydrostatic axisymmetric numerical model. *J. Atmos. Sci.,* **44,** 542–561.

Simpson, R. H., and H. Riehl, 1981: *The Hurricane and Its Impact.* Louisiana State University Press, 398 pp.

Velasco, I., and J. M. Fritsch, 1987: Mesoscale convective complexes in the Americas. *J. Geophys. Res.,* **92,** 9591–9613.

Williams, M., and R. A. Houze Jr., 1987: Satellite-observed characteristics of winter monsoon cloud clusters. *Mon. Wea. Rev.,* **115,** 505–519.

Zehnder, J. A., and R. L. Gall, 1991: On a mechanism for orographic triggering of tropical cyclones in the eastern North Pacific. *Tellus,* **43A,** 25–36.

Zehr, R., 1976: Tropical disturbance intensification. Dept. of Atmospheric Science Paper 259, Colorado State University, Ft. Collins, CO, 91 pp. [Available from Dept. of Atmospheric Science, Colorado State University, Fort Collins, CO 80523.]